USE OF CLOUD ANALYSES TO VALIDATE AND IMPROVE MODEL–DIAGNOSTIC CLOUDS AT NMC

Kenneth A. Campana
National Meteorological Center
Washington, D. C. 20233

1. INTRODUCTION

Several operational numerical weather prediction models are used at the National Meteorological Center, Washington (NMC – soon to be NCEP, the National Centers for Environmental Prediction, see McPherson, 1994). A T126 global, spectral, medium–range forecast (MRF) model (Kalnay, et al., 1990) is used for 10 day and longer predictions, and both a regional nested grid model (NGM – see DiMego, et al., 1992) and a mesoscale (Eta) model (Black, 1994) are used for shorter range forecasts. The MRF and Eta models use a radiation parameterization developed at the Geophysical Fluid Dynamics Laboratory (GFDL) by Fels and Schwarzkopf (Table 1). Longwave (LW) and shortwave (SW) radiation are computed every 3 hours in the MRF model, and every 2 and 1 hour, respectively, in the Eta model. The diurnal cycle is approximated via a cosine solar zenith angle weighting at each model time step.

Clouds exert strong influences on the radiative processes in the atmosphere, which, in turn alter both the atmospheric thermal structure and the processes near the earth's surface. Currently (Autumn 1994), clouds in the MRF model are diagnosed from model data (Slingo, 1987 and Campana, 1990) and range in fractional value from 0.0–1.0 for Low, Middle, and High (L, M, H) cloud types. Stratiform clouds primarily are based on relative humidity (RH), with onset of cloudiness occurring at RH=0.8 for all types. Generally, clouds are not allowed in the lower 10% of the atmosphere, except in suspected marine stratus environments, where moist layers exist beneath a low–level inversion capped by dry air (Kanamitsu et al., 1991). Convective clouds are diagnosed from model convective precipitation rate (Slingo, 1987), where tops and bases are obtained from the convective parameterization. Unification of cloud–related processes, via use of a cloud water variable (Zhao, 1994), is being implemented in the regional Eta model.

This report focuses on use of available global cloud analyses to validate and to improve the diagnostic cloud formulation in the MRF model. The next section discusses the global cloud analyses that are available to NMC in quasi real–time (within 48 hours of observation time). Section 3 discusses the routine validation of MRF clouds that has been done over the past several years. The subsequent three sections discuss improvements made to the MRF diagnostic cloud scheme, with specific emphasis on the method employed to tune the stratiform cloud formulation. Future plans at NMC envision more complete regional investigations of the modeled clouds, a new SW parameterization, which will model cloud and (new) aerosol effects more realistically, and experimentation with Zhao's (1994) Eta model explicit cloud prognostic scheme in the MRF. The work reported here evolved from the valuable assistance of many colleagues and their contributions are gratefully acknowledged below each section title.

2. CLOUD ANALYSES

(K. Campana, K. Mitchell, Y. Hou, S. Yang, NMC and L. Stowe and L. McMillin, NESDIS)

A number of global cloud analyses have become available at NMC over the last several years. In mid–1992, NMC began to receive the United States Air Force (USAF) Real–Time Nephanalyses (RTNEPH, see Hamill, et al., 1992) 4 times daily via the DOD/NOAA–NESDIS Shared Processing Network. Additionally, NMC has been interacting with scientists at NOAA/NESDIS as they develop improved cloud products, both from multi–spectral AVHRR data and TOVS sounder data. The latter two algorithms, still under development, are currently run in an experimental/operational mode.

The RTNEPH clouds are placed on polar stereographic grids of the northern and southern hemispheres, where the horizontal resolution is 47.625 km at 60 degrees latitude. Data sources are primarily the infrared (IR) and visible (VIS) channels on two DMSP satellites, with some information obtained from NOAA 11/12; however, surface observations are used significantly when available, and a manual bogus is employed during each analysis cycle. The RTNEPH dataset consists of total cloud and up to 4 distinct layered

TABLE 1. Radiation Parameterization (GFDL) in NMC's MRF Model

	Spectral region	Process	Comment
Clear Sky	Longwave	Gas absorption	0–2200 cm^{-1} region
		H_2O	Hybrid scheme separates the exchange between layers and the cooling to space (CTS) terms (Schwarzkopf and Fels, 1991). CTS term calculated using 10^{-1} cm bands, combined into 8 bands over the 160–560 cm^{-1} region. Exchange term is calculated using wide–band emissivity formulation.
		H_2O continuum	Extended region, 400–1200 cm^{-1} (Schwarzkopf and Fels, 1991 and Roberts et al., 1976).
		CO_2 and H_2O	CO_2 transmission from pre–tabulated functions, over 560–800 cm^{-1} region, 2 bands used in CTS calculations (Schwarzkopf and Fels 1991, 1985), where CO_2=330 ppmv.
		O_3	One interval random band model (Rodgers, 1968), where O_3 = seasonal zonal mean.
	Shortwave	Gas absorption	12 subintervals covering the solar spectrum
		O_3	Analytic formula: Lacis and Hansen (1974)
		H_2O	Lacis and Hansen (1974), modified to 12 bands.
		CO_2	Formula of Sasamori et al., 1972
		Rayleigh scattering	Effects on O3 (Lacis and Hansen, 1974)
		Diurnal cycle	Radiative flux calculation using daylight mean cosine solar zenith angle. Values weighted by actual cosine zenith angle at each model grid point and time–step.
		Surface albedo	Land: background from SiB climatology (Dorman and Sellers, 1989), altered for snow. zenith angle dependent if not snow. Ocean: zenith angle dependent (Payne, 1972) Sea ice: background=0.5, altered for snow.
Cloudy Sky		Cloud overlap	Random
	Longwave	Scattering	None
		Absorption	Low, Middle cloud black (emissivity=1.) High cloud emissivity varies linearly with latitude, from 0.6 in tropics to 0.3 at poles.
	Shortwave	Scattering	Preset albedo for low, middle, and high cloud (Manabe and Strickler, 1964)
		Absorption	Preset absorptivity as above.
		Multiple refections	Among cloud layers and earth's surface.

clouds, where each grid point contains cloud coverage, geopotential height of the layered cloud bases and tops, time of observation, and diagnostic information. Routine monitoring of RTNEPH data receipt was performed at NMC during September 1993–May 1994, and it showed that less than 10% of the Shared Processing Network transmissions were missing or shortened due to problems at either the originating or receiving locations. Generally, over 80% of the analysis data points were valid within 3 hours of synoptic observation time and it was rare to find more than two distinct cloud layers (only 6 and 1 percent of the data had three or four cloud layers, respectively). Hamill et al. (1992) note that the intent of the RTNEPH is to maximize the probability of cloud detection, so there is a tendency to over–estimate both clear and overcast conditions, while under–estimating partly cloudy situations. They also note several RTNEPH limitations – *e.g.* the IR satellite cloud–retrieval is a one–channel infrared algorithm, so when no VIS data is available, there is a tendency to miss warm low stratus cloud as well as to underestimate high thin cirrus cloud, or to falsely place cirrus too low in the atmosphere. There are plans to improve the operational RTNEPH (*e.g.* multi–spectral techniques) by the end of the decade.

Figure 1 shows monthly mean cloud fraction from the RTNEPH for July 1994 and from the ISCCP (International Satellite Cloud Climatology Project, Schiffer and Rossow, 1985) for July 1985.

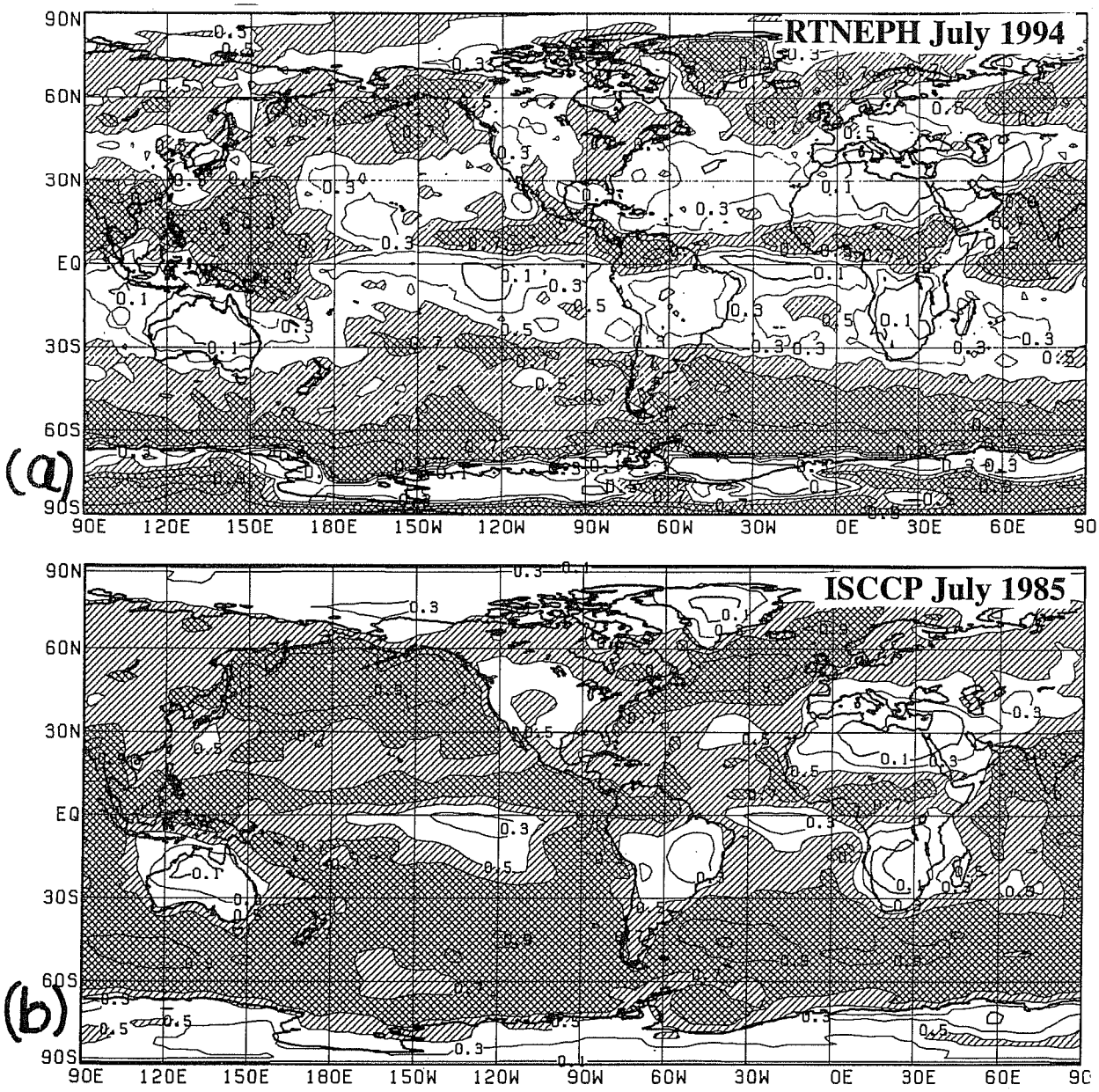

Fig. 1 Monthly mean total cloud fraction, contour interval 0.2, shaded > 0.5, cross–hatched > 0.7 a) RTNEPH July 1994, b) ISCCP July 1985.

Though for different years, these monthly means generally agree in the locations of major atmospheric features; however, the ISCCP data, with a global cloud fraction of 0.63 is significantly cloudier than that of the RTNEPH (0.49). Some "in–house" NMC comparisons show that the RTNEPH is more similar to Nimbus–7 data (July mean cloud fraction is 0.52), though those clouds are considered "uniquely" lower in fractional coverage relative to other cloud climatologies (Mokhov and Schlesinger, 1994).

NMC is also receiving total cloud fraction from NOAA/NESDIS in quasi real–time. The completely satellite–derived product is from the CLouds from AVHRR (CLAVR) algorithm (Stowe, 1991) and is available on a 1 degree global grid for both ascending and descending orbits. CLAVR is a multi–spectral cloud detection algorithm based on a sequence of threshold tests which differ for land, sea, day, and night. Tests include intensity discrimination against the background, multi–spectral differences and ratios, and spatial uniformity in the 2x2 pixel arrays. CLAVR clouds differ from its RTNEPH counterparts, not only because the algorithm does not use conventional surface information over data–rich land regions, nor does it sample as frequently in time, as the RTNEPH, but also because its threshold tests allow a more accurate sensing of thin cirrus and low stratus (Hou et al., 1993). While the RTNEPH attempts to maximize the probability of cloud

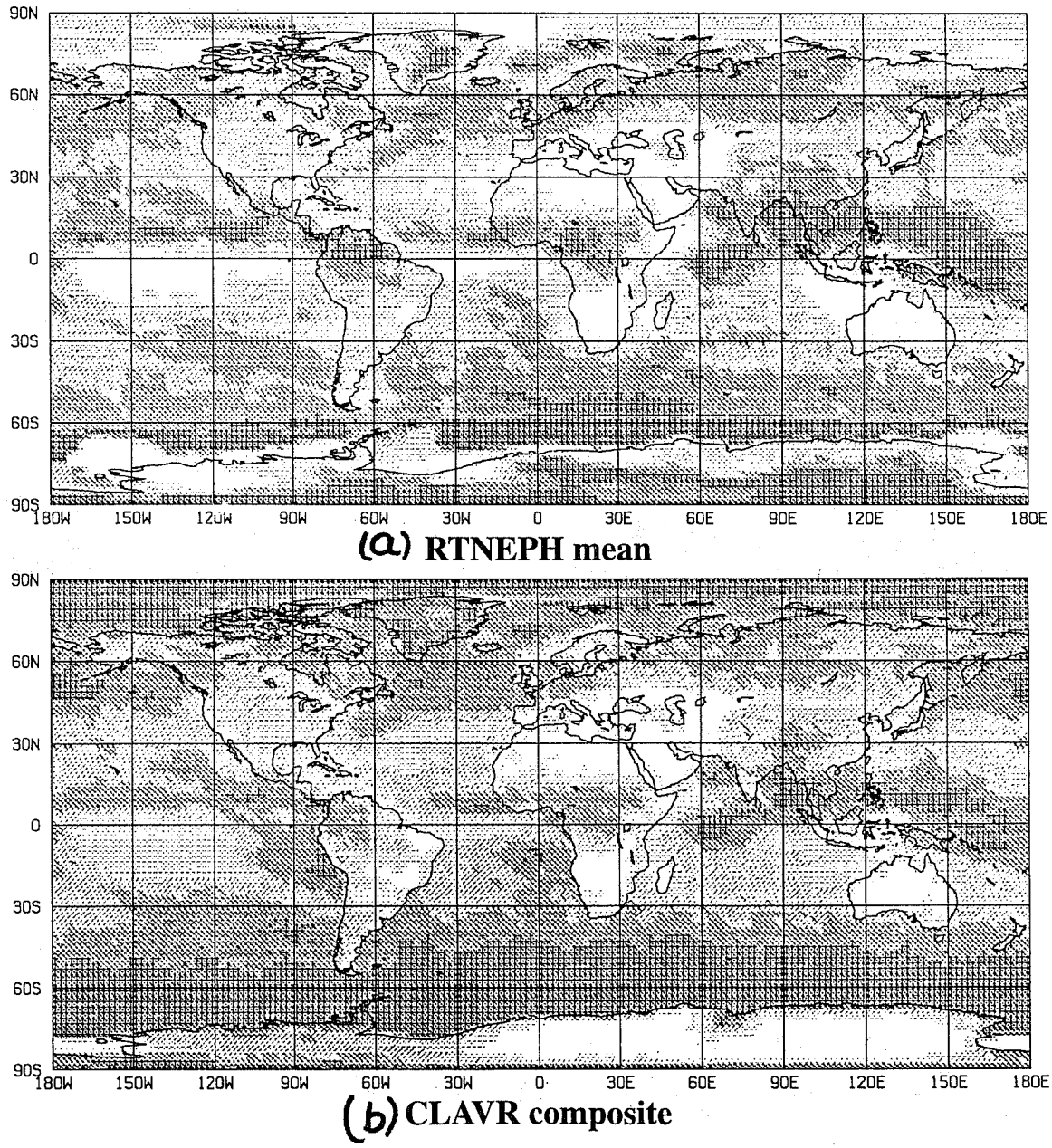

Fig. 2 Total cloud fraction for 1–13 September 1994. Interval every 0.2
a) RTNEPH mean, b) CLAVR composite.
Dark=0.8 – 1.0, White=0–0.2

detection, the current CLAVR algorithm overestimates the frequency of occurrence of partly cloudy situations – frequency distributions of its clouds peak near a fractional value of 0.5 (Hou, et al., 1993). Future CLAVR development will soon improve cloud fractional coverage and produce cloud in up to 3 distinct layers.

Figure 2 compares mean total cloud fraction from the RTNEPH analysis and composited CLAVR cloud fraction from ascending and descending orbits of NOAA 11, both for the same 12 days in September 1994. The CLAVR global mean of 0.56 is larger than the RTNEPH mean of 0.51, and appears to result from the less sharp CLAVR distinction between clear and overcast regions caused by the tendency to produce partly cloudy values near 0.5. Both data sets 'suffer' in regions poleward of 60 degrees. While it is difficult to verify, it appears that the low stratus off South America and south Africa in CLAVR is more realistic (see Heck et al., 1990 for some information on summertime climatology in these regions). The Inter–Tropical Convergence Zone (ITCZ) seems less defined in CLAVR over land masses, however the RTNEPH may overestimate tropical cloud. Detailed comparison of individual ascending and descending orbital data (where RTNEPH data has been spatially and temporally,+/–3 hours, interpolated to CLAVR orbital paths) shows excellent agreement between the two datasets (Fig. 3) except in regions where the RTNEPH is deficient. That is, after reviewing channel brightness temperatures, the CLAVR detection of low cloud between 150W–165W in Fig. 3 appears to be more accurate.

Other NOAA/NESDIS satellite–derived global cloud products available to NMC are the effective cloud cover (physical cloud fraction 'times' emissivity) and cloud–top pressure from TOVS sounder data (McMillin et al., 1994). Comparison of a TOVS cloud composite with mean RTNEPH cloud for the same

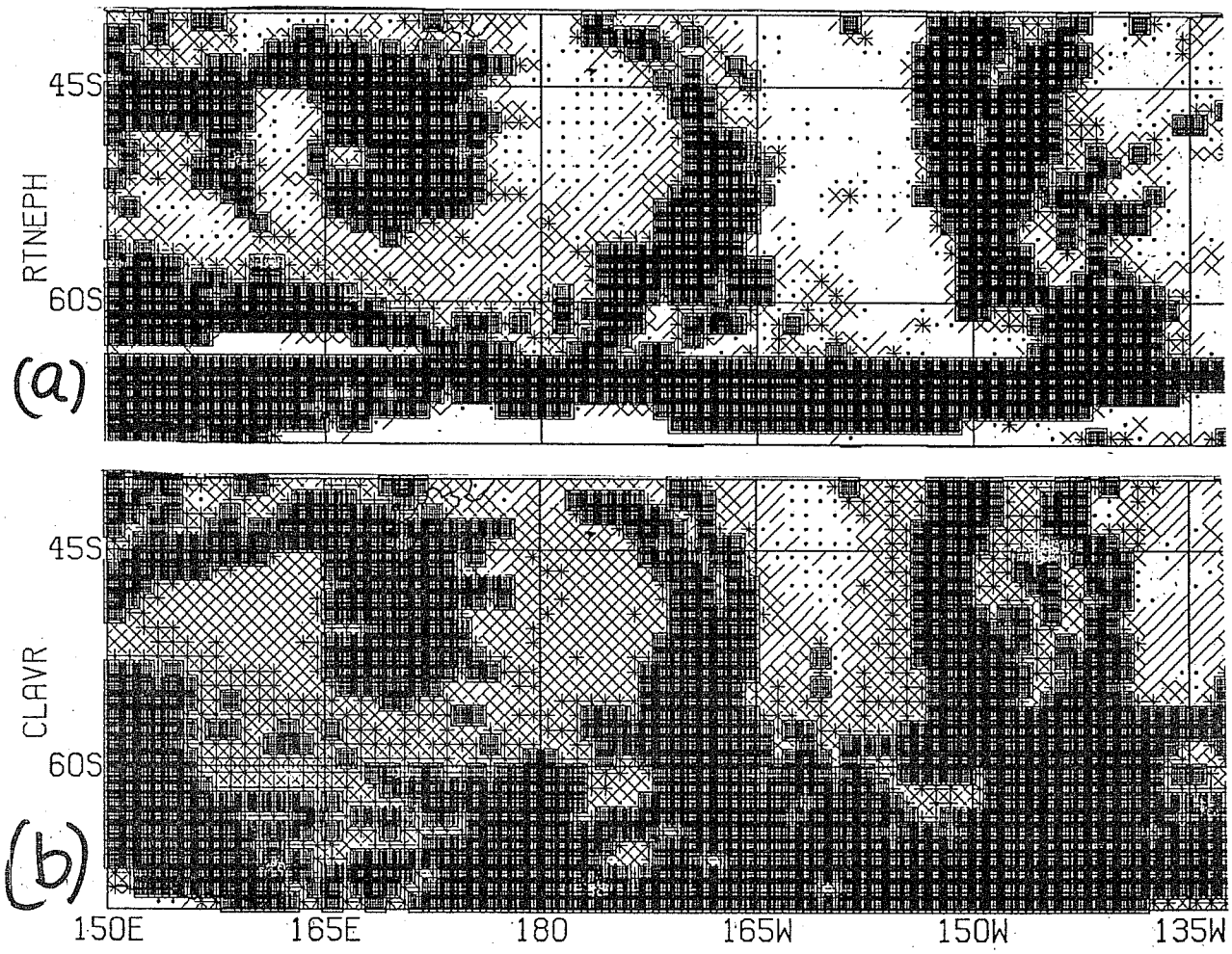

Fig. 3 Total cloud fraction in southern hemispheric ocean region (40S–65S) for 11 September 1994, RTNEPH (top) and CLAVR (bottom). RTNEPH data spatially and temporally (3 hour window) interpolated to ascending CLAVR orbits. Dark=0.9–1.0, White=0–0.1, interval every 0.2

18 days in September 1994 shows general agreement in latitudinal structure (Fig. 4); however, TOVS has much less cloudiness, in part due to cloud emissivities of less than 1. The ITCZ cloudiness is especially weak. This may result from an inability to obtain the clear–sky radiances needed for the cloud retrieval algorithm in regions of persistent precipitation (thus leaving only the less cloudy pixels to be sampled). Marine stratus cloud located off South America and south Africa is quite evident in TOVS and, as in CLAVR, is probably more correct than the RTNEPH. However TOVS may suffer from nighttime excess cloud over desert regions.

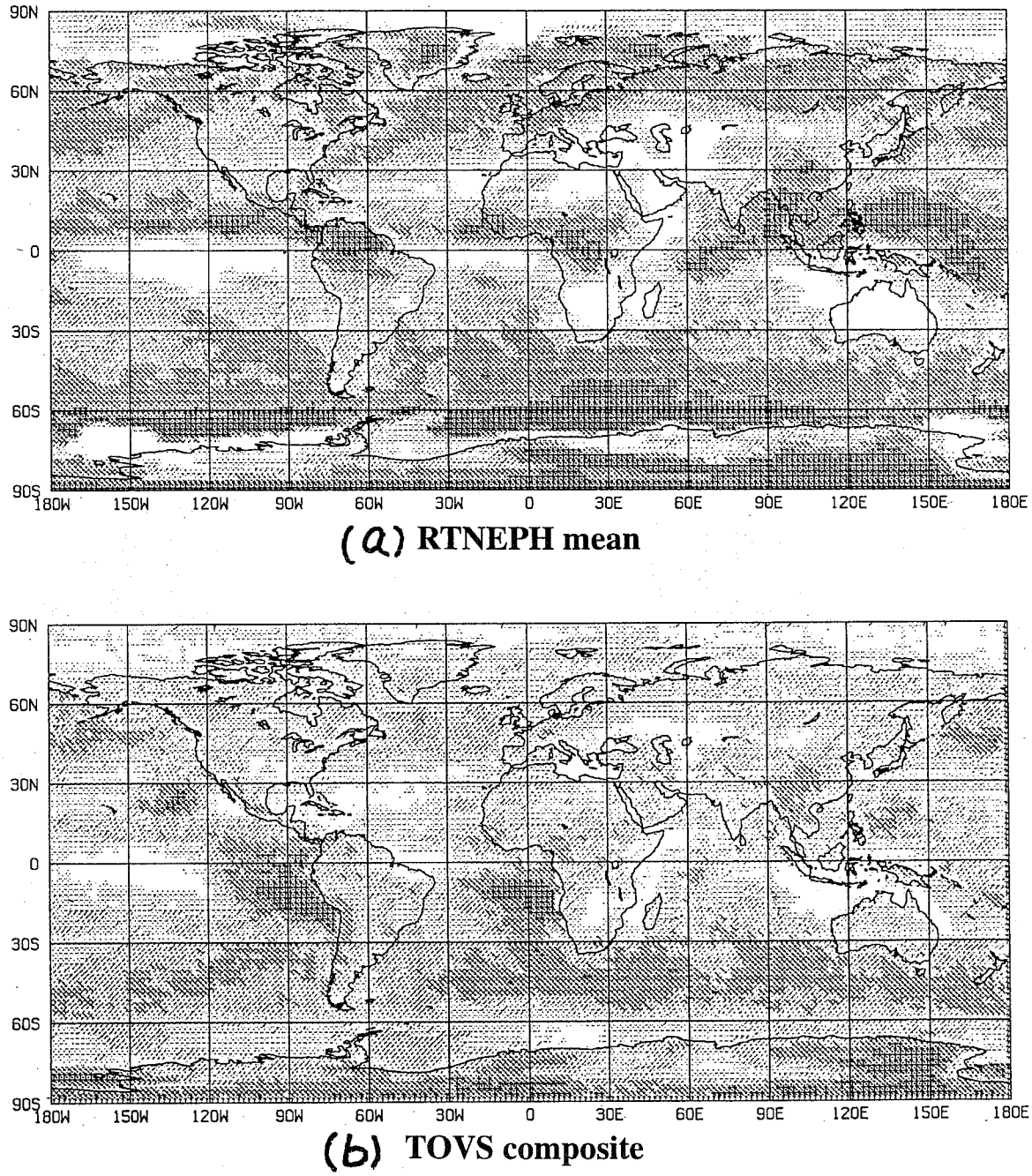

Fig. 4 Total cloud fraction for 18 days during 2–30 September 1994. Interval every 0.2 a) RTNEPH mean, b) TOVS composite. Dark=0.8–1.0, White=0–0.2

3. VALIDATION OF MODEL CLOUDS

(K. Campana, K. Mitchell, Y. Hou)

For NWP purposes, cloud validation should be made in both quasi real–time for routine diagnosis, and retrospectively, on specific data sets, for more completeness. Major data sources for the former are conventional surface/upper air observations and satellite retrievals, and for the latter are global datasets such as ISCCP, special collections such as TOGA–COARE, and field experimental data from radar and aircraft (to validate cloud microphysics). Satellite–sensed products can be conveniently typed as: a) raw radiances and b) processed cloud fractions / radiative fluxes. The advantage of the first is that any discrepancy between model and satellite is generally a model error (*i.e.* there is no error introduced due to a satellite retrieval algorithm). The advantage of the second type is that its in an easier form for the atmospheric modeler to use. However, the algorithms which process raw satellite data are fraught with their own problems (recall the difficulties with the RTNEPH noted by Hamill et al., 1992), and its often difficult to "know " the true state of the cloud field, as Figs. 1–4 demonstrate. Additionally, use of radiative fluxes as a surrogate for a physical cloud analysis may prove difficult to interpret, as one must unravel effects of the fractional amount, thickness, top of clouds as well as temperature and moisture in the atmospheric column. Of course, inherent to any model–cloud validation effort is an assessment of the realism exhibited by the predicted 3–dimensional moisture field, since it is the ultimate driver of the cloud parameterization.

Verification of model clouds may be accomplished in several manners. Point verification of clouds can be made relative to surface observations. Parameters easily compared are total cloud fraction and cloud base information, as well as the near–surface environment; however, this requires frequent saving of model data at a number of grid points. Most NWP centers are already using such model data to construct station time series or 'meteograms'. Global verification requires satellite data, and to properly validate clouds, one should interpolate model data to the approximate space/time location of the satellite observations (Hou et al., 1993). The cloud parameters most easily compared include total (and perhaps layered) cloud fraction, cloud top height, and cloud properties (using top–of–the–atmosphere, TOA, radiation). This requires frequent (hourly?) saving of a model's 3–dimensional cloud structure and may be prohibitive on a routine basis. We have adopted a somewhat less ambitious validation effort for the NMC global model, one which will provide information needed to estimate how well the MRF clouds are parameterized. Daily mean 'observations' from RTNEPH and CLAVR data are used both to identify geographical regions where there are MRF cloud forecast problems and to assess the impact, on the cloud parameterization, of changes to other components of the MRF model. Methods employed in this paper make use of gridded cloud fields as well as USAF–developed statistical scores.

The RTNEPH clouds are stored on a 31–day rotating disk as equal–angle gridded 1–degree H, M, L and total cloud fractions, in order to use them, conveniently, after the real–time MRF forecasts are complete. During this processing, the original RTNEPH hemispheric synoptic data (stored on a 7–day rotating disk) pass through a rudimentary quality control step, which both restricts the cloud information to a 3–hour window encompassing each 6–hour synoptic time and requires cloud fraction, top/base height, and cloud type, all, to have realistic values. Pressure boundaries are used to define the H, M, L domains in a fashion similar to the MRF model. They are latitudinally dependent, with the pressure defining the boundary between L and M cloud (M and H cloud) being 65 cb (45 cb) equatorward of 45 degrees latitude and linearly increasing to 75 cb (55 cb) at the poles. A higher pressure value, than in the MRF, is necessary for the boundary between the M and H domains in order that sufficient H cloud can be found (recall that high cloud is difficult for the RTNEPH to detect and is usually placed too low in the atmosphere). The vertical compaction into H, M, L is performed first. Geopotential heights of the domain boundaries are obtained hydrostatically from analyzed temperatures (at the desired synoptic time), which have been horizontally interpolated from the MRF model grid to the RTNEPH grid. Then the H, M, L and total cloud fractions are horizontally compacted to the 1 degree grid, using a binning procedure in regions where the polar stereographic grid horizontal resolution (approx. 47 km) is small relative to the 1 degree grid, and using a linear interpolation, in polar regions, where it is not.

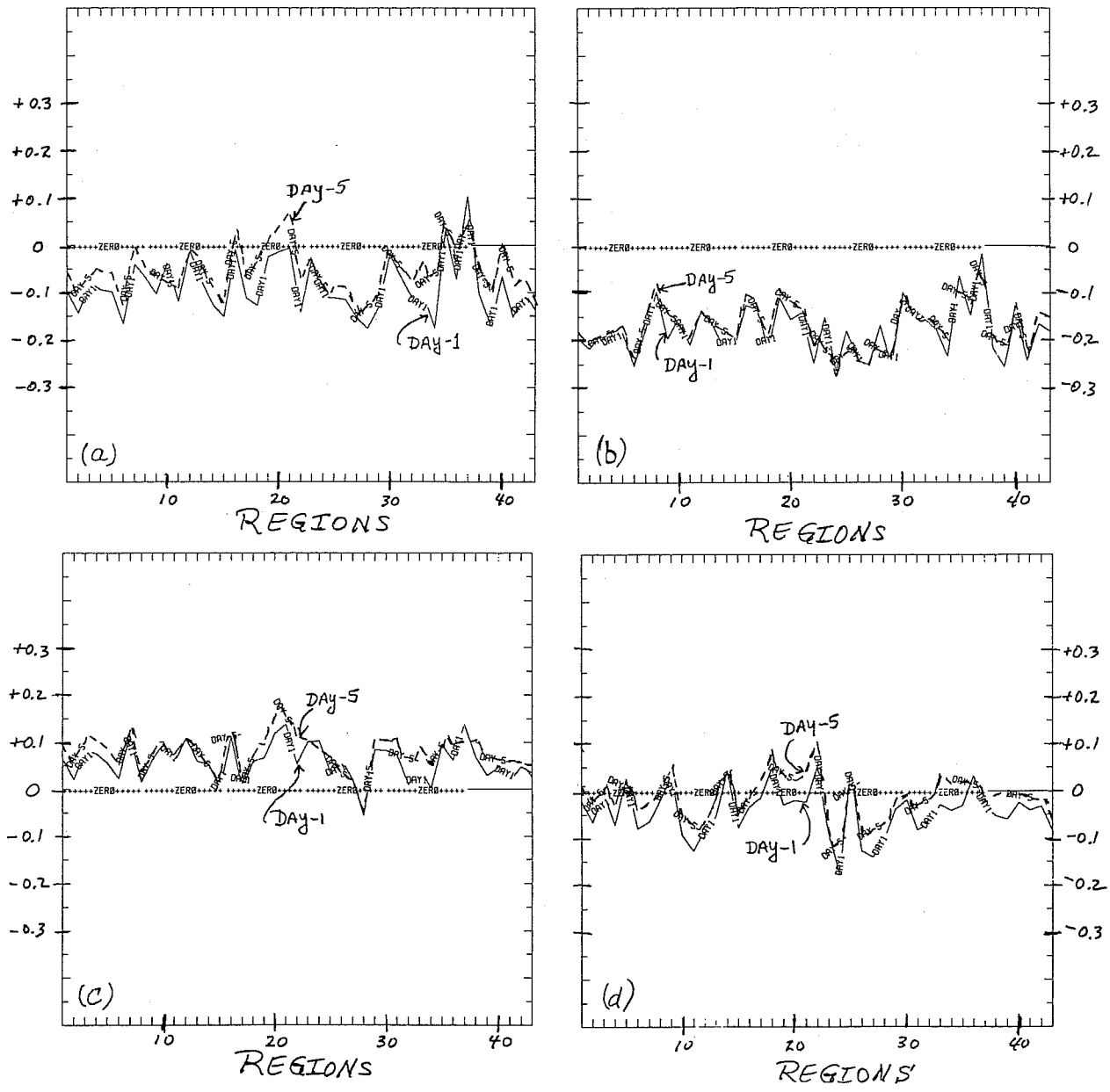

Fig. 5 Bias scores (43 regions) for MRF model (T126L28) .vs. RTNEPH daily mean analyses in August 1994 – forecast day–1 (solid) and day–5 (dashed). Regions 1–3 are global (all points, land points, ocean points), 4–9 are for northern and southern hemispheres, . . . ,38–43 are for eastern/western North America and South America (all points and land points)
a) total cloud, b) low cloud, c) high cloud, d) middle cloud.

Following the practice of Mitchell and Hahn (1989), a set of USAF statistical scores documented in Trapnell (1992), and modified by Hou et al. (1993), is used to validate the model's H, M, L, and total cloud. Scores are calculated from 2–dimensional contingency tables of cloud fraction, obtained from both RTNEPH daily–mean analyses (interpolated to model grid from the 1 degree analysis) and MRF model daily mean forecasts, for a set of 43 regions covering the globe. In limited cases, the same is done using composited daily mean CLAVR total cloud fraction. The regions range from fully global (regions 1–3) to smaller ones such as eastern North America land points (region 39). Several of the regions are listed in the Fig. 5 caption. The contingency tables consist of 11 cloud fraction categories: 0–.05, .05–.15,..., .85–.95, .95–1. Scores used in this paper are traditional ones, such as bias and correlation, as well as less traditional 20/20 and contrast scores. The USAF 20/20 score, ranging from 0 to 1, provides a measure of how well two gridded cloud fields agree – its value represents the fraction of points where cloud fractions differ by less than 0.2 (a value of 1 means perfect agreement within 0.2). The contrast score, ranging from 0 to 1, measures the sharpness of the

gradient between clear and overcast regions – its value is a measure of similarity to a "U–shaped" cloud frequency distribution, where a value of 1 means a perfect binary distribution (cloud fractions either 0 or 1) and a value of 0 means a perfectly flat distribution (cloud fractions are constant).

Bias scores for individual forecasts during August 1994 are typical of monthly validations performed over the last year, and they show that the model underestimates total cloud by order 0.1 globally (leftmost region on Fig. 5). The global underestimate by the MRF is quite serious, considering that the RTNEPH, itself, may be an underestimate (see section 2, in conjunction with Mokhov and Schlesinger, 1994). The MRF model underestimate is regional in character (regions 22–29 on Fig. 5 include Asia, Australia, Western Pacific and Indian oceans) and it is dominated by an especially large model underestimate of low cloud. On the other hand, high cloud is overestimated, though RTNEPH observed H cloud, itself, may be underestimated. The two curves represent day–1 and day–5 MRF forecasts, and model spinup toward more cloudiness (represented as an increase in bias) is primarily due to an increase in predicted relative humidity at middle and high latitudes in the M and H domains.

Correlation scores also show a regional effect (Fig. 6) and generally drop significantly by the day–5 forecast. Recalling section 2, there is uncertainty in knowing the "true" cloud state; however, one can

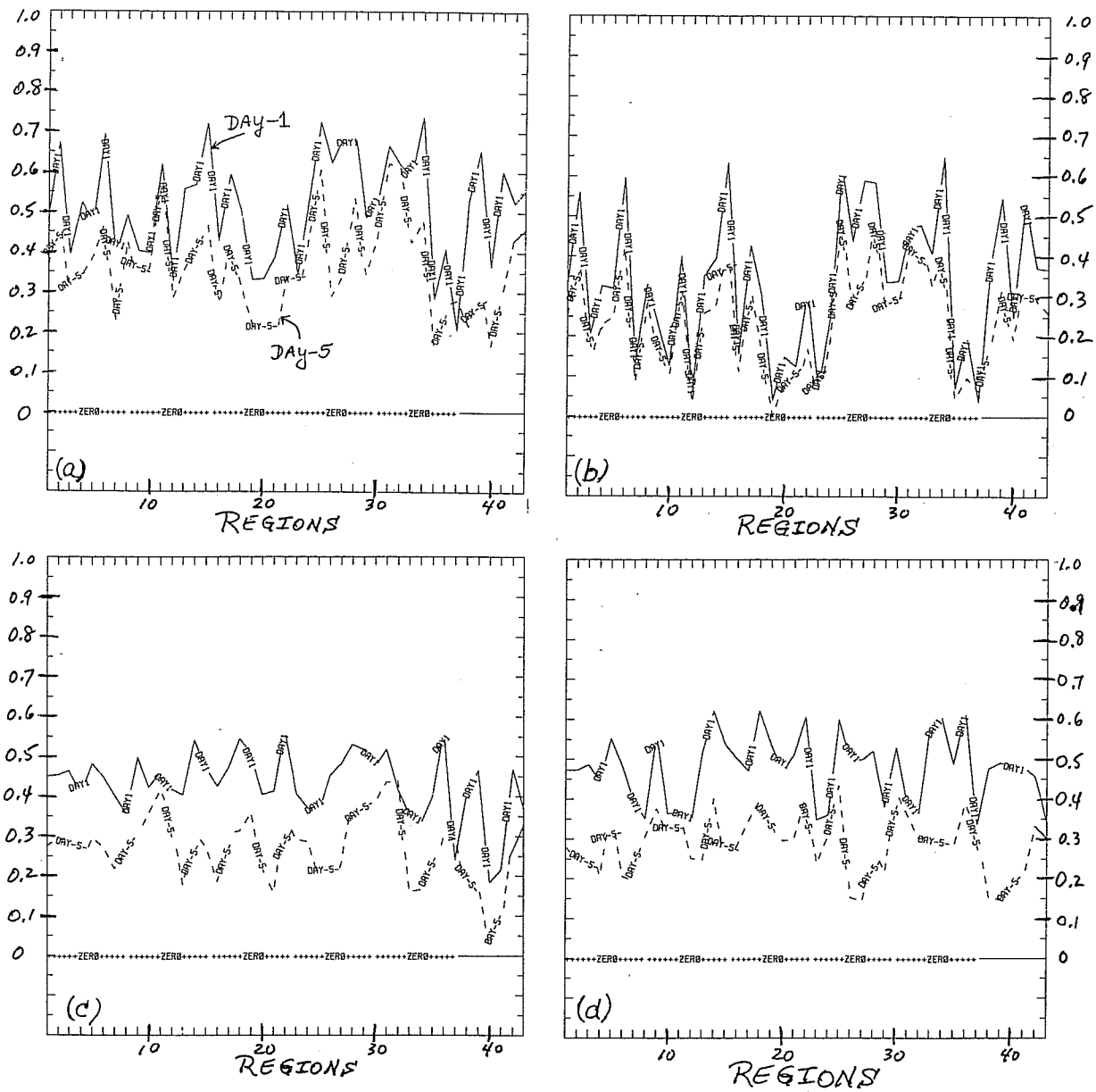

Fig. 6 Correlation scores (43 regions) for MRF model (T126L28) .vs. RTNEPH daily mean analyses in August 1994 – forecast day–1 (solid) and day–5 (dashed).
a) total cloud, b) low cloud, c) high cloud, d) middle cloud.

estimate the magnitude of a good correlation by comparing two independent cloud analyses, valid at the same time. Fig. 7, obtained by correlating CLAVR with the RTNEPH total cloud during August 1994, suggests that a good regional correlation ranges between 0.7–0.8. Illustration of the difficulty in validating model clouds, due to uncertainties in observed cloud coverage, is evident in contrast scores for RTNEPH and CLAVR (dashed lines in Figs. 8a and 8b, respectively). Here, the the higher scores imply that the RTNEPH has sharper gradients between clear and overcast areas than does either the CLAVR or the MRF; the latter is evident in the 2–dimensional depiction (Fig. 19). Contrast scores for MRF model cloud forecasts at day–1 are closer to CLAVR (Fig. 8b) than the RTNEPH (Fig. 8a).

Routine statistical verification of MRF clouds is similar for each month (Fig. 9). The maximum bias score is +0.2 in the equatorial Atlantic (15N–15S) where the lowest correlation (0.10) occurs. This is a region of persistent MRF–modeled low stratus, which may exist in reality, but it is not detected by the RTNEPH product. The minimum bias of –0.15 occurs primarily over land areas, where surface station ob-

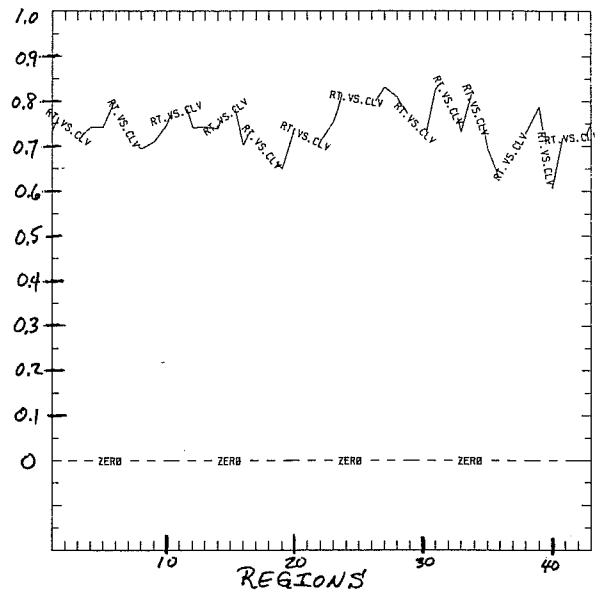

Fig. 7 Correlation scores (43 regions) for CLAVR daily composite .vs. RTNEPH daily mean total cloud in August 1994.

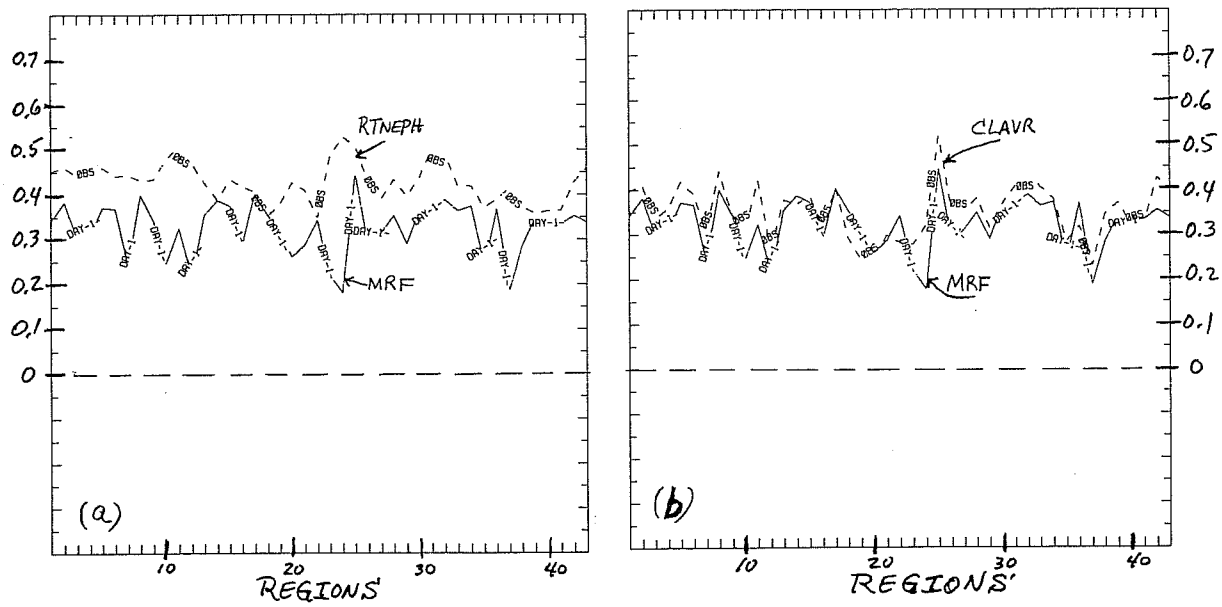

Fig. 8 Contrast scores (43 regions) total cloud for MRF model day–1 forecast (solid) .vs. cloud analysis (dashed) in August 1994. The MRF curves are the same in both figures.
a) cloud analysis = RTNEPH, b) cloud analysis = CLAVR.

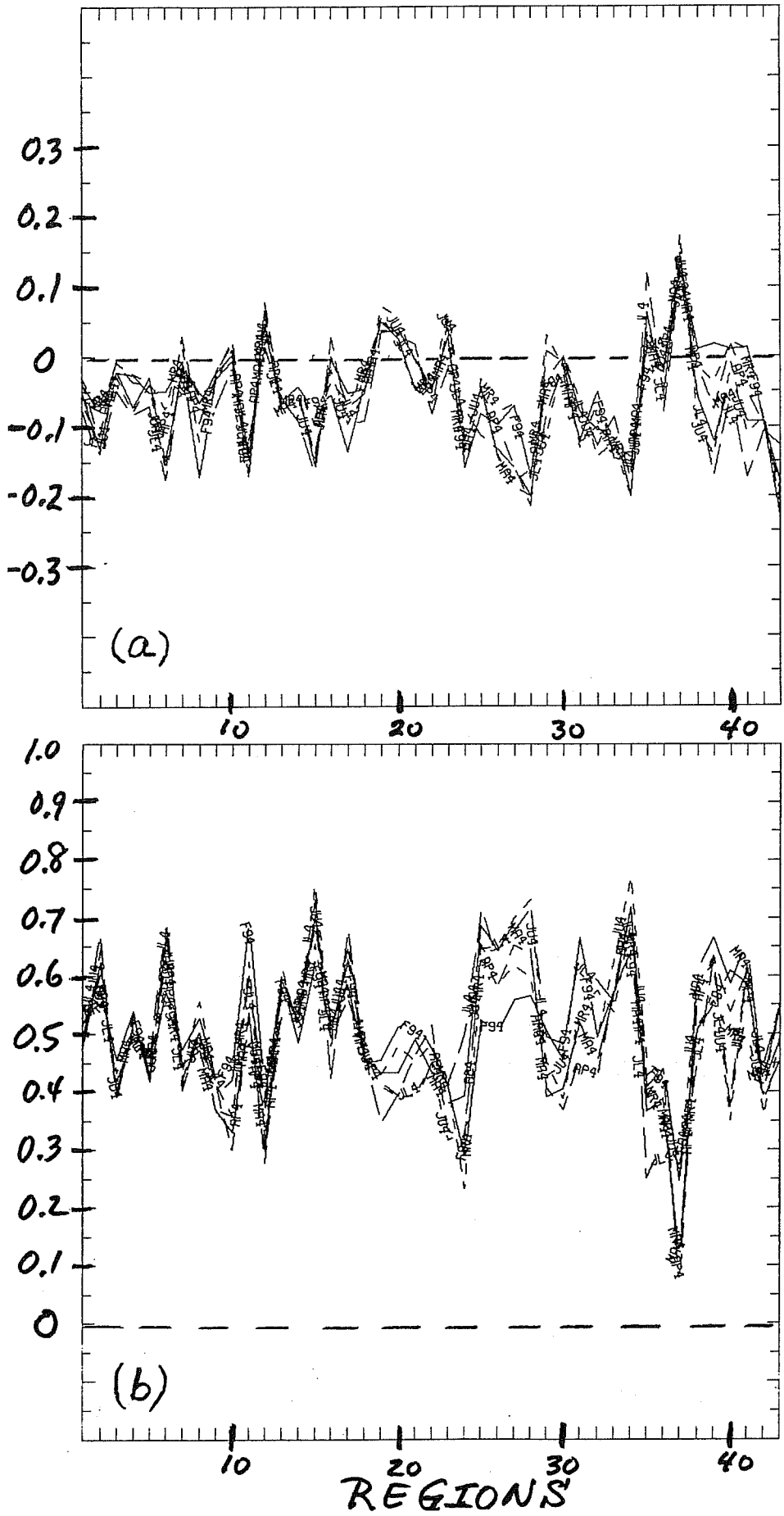

Fig. 9 Regional scores (43 regions) for MRF model (T126L28) .vs. RTNEPH daily mean total cloud for 6 months, February–July 1994 – forecast day–1.
a) Bias, b) Correlation.

servations undoubtedly improve RTNEPH detection of low cloud. There are some seasonal variations, especially in the Australian/east Asian regions where the ITCZ moves across the equator (regions 25–28), but, generally, scores are quite persistent. This implies that the MRF model analysis and forecast system is able to simulate qualitative seasonal changes in atmospheric moisture quite well, and that any variations in cloud scores are driven by model convective processes. Thus, MRF cloud forecast results obtained from limited testing of new MRF diagnostic–cloud schemes may be generalized to larger sample (test) sizes.

The RTNEPH monthly mean total cloud analyses show a distinct movement of the ITCZ across the equator between July 93–February 94–July 94 (Fig. 10a–c). The mean MRF total cloud for forecast day–1 is realistic in this movement (Fig. 10d–f), but it underestimates cloud fraction and lacks some of the RTNEPH details. In July 1993, the MRF was a T126 18–layer model with Kuo convective parameterization, and its cloud depiction appears quite spotty. After July 1993, the MRF changed to a 28–layer model with a modified Arakawa–Schubert convective parameterization. Its cloud depiction in July 1994 is significantly better; however, as seen later, this appears to be due to overestimating high cloud relative to the RTNEPH.

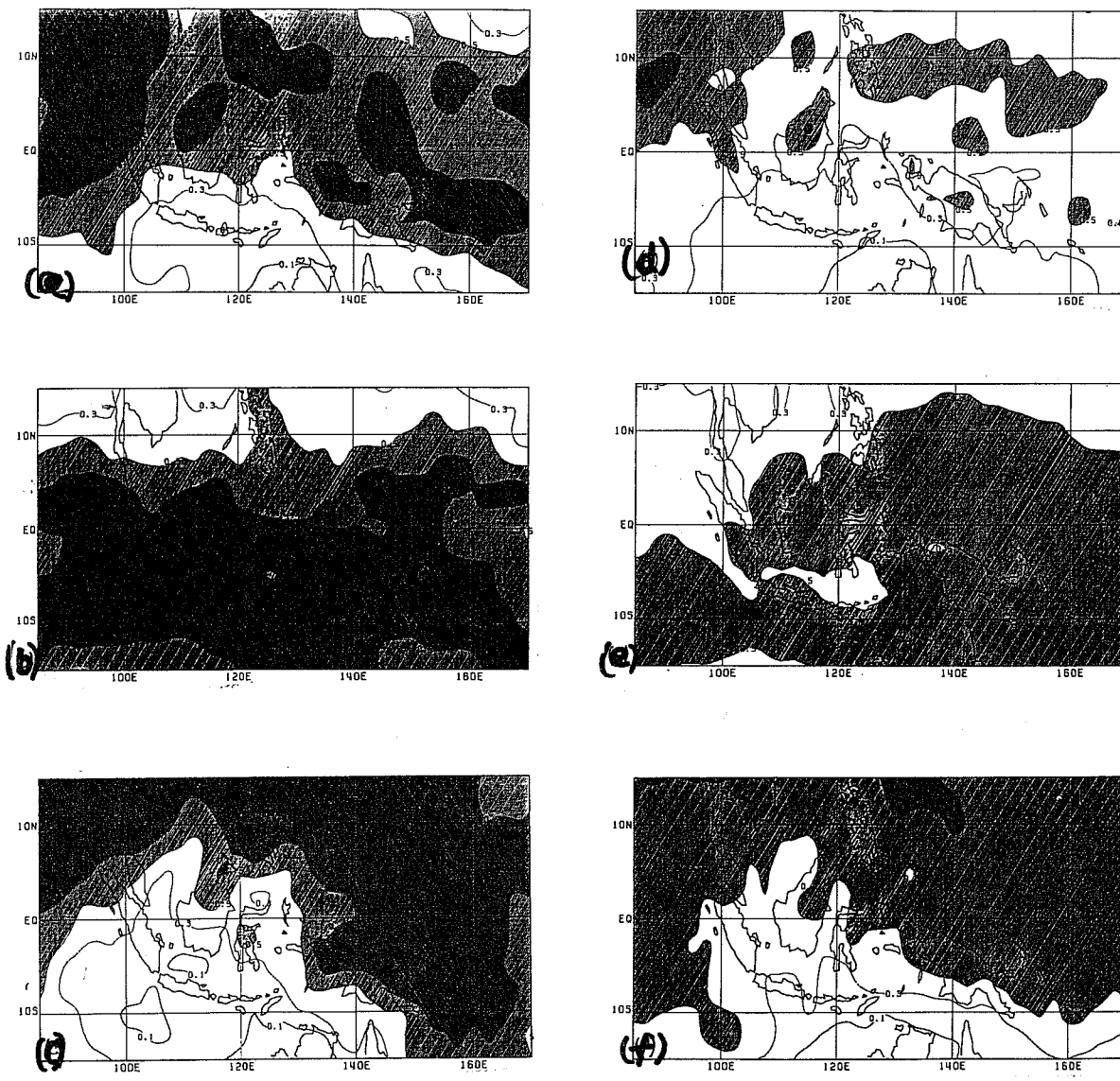

Fig. 10 Monthly mean total cloud fraction for 90E–170E, 15N–15S (MRF model data is for forecast day–1), contour interval 0.2, shaded > 0.5, cross–hatched > 0.7.
a) RTNEPH July 1993, b) RTNEPH February 1994, c) RTNEPH July 1994,
d) MRF (T126L18, Kuo) July 1993, e) MRF (T126L28, Arakawa/Schubert) February 1994,
f) MRF (T126L28, Arakawa/Schubert) July 1994.

4. TUNING THE CLOUD/RELATIVE HUMIDITY RELATIONSHIPS
(K. Campana, K. Mitchell)

A number of deficiencies in the MRF model's cloud and radiation fields are documented in Campana et al., 1990, Cullather, 1993, and Campana et al., 1994a. Among them are underestimates of cloud coverage, especially for land areas and for oceanic low cloud, and overestimates of both outgoing longwave radiation (OLR) at the top–of–atmosphere and downward shortwave radiation (DSW) at the earth's surface. Since the model produces realistic forecasts both of middle/high latitude weather systems and, in a qualitative sense, of clouds, (and, by implication, the forecasted 3–dimensional moisture structure), one should be able to remove some of the deficiencies in modeled cloud by tuning the MRF diagnostic cloud scheme to observational data.

An objective method, developed by Mitchell and Hahn (1989, 1991), and further tested by Trapnell (1992), is chosen to tune the model's stratiform cloud/RH relationship to observed data. The scheme preserves several statistical properties of the chosen cloud analyses in the cloud/RH relationships, assuming a high correlation between RH and the occurrence of stratiform cloud, by mapping cumulative frequency distribution of observed cloud to the forecast model's RH distribution. Frequency distributions of both forecast model RH fields and observed cloud fraction are calculated in 0.01 bins for the same valid time on the same horizontal domain. Then the cumulative frequency distribution of the cloud analysis is projected, or mapped, onto that of the RH data, yielding both a quasi–continuous specification of cloud fraction as a function of model RH as well as an objective estimate of the "critical" RH, value, which signifies the onset of diagnosed cloudiness. An analogous objective method has been independently developed by Rikus and Hart (1988).

The observed cloud used is the 1 degree daily mean H, M, L RTNEPH data described in section 3, and the model RH data used is the maximum layer values within the same H, M, L domains. The Mitchell and Hahn method has been used over the past year and a half to develop cloud/RH relations for the T126 MRF model. The data has been stratified by surface type (*e.g.* land, sea), by geographical region (*e.g.* tropics, mid–latitude), by forecast day, by vertical location (*e.g.* H, M, L), and, in a limited sense, by types of cloud observation (*e.g.* ISCCP, daily mean RTNEPH, synoptic RTNEPH). An alternative stratification of data by synoptic region has been reported by Nehrkorn and Zivkovic (1994).

A number of expected sensitivities have been noted in the computed cloud/RH relationships, and several representative examples are shown in Figs. 11–13. Differences in choice of verifying observational analyses (Fig. 11) have a large impact on the computed relations, as seen for low cloud in the northern

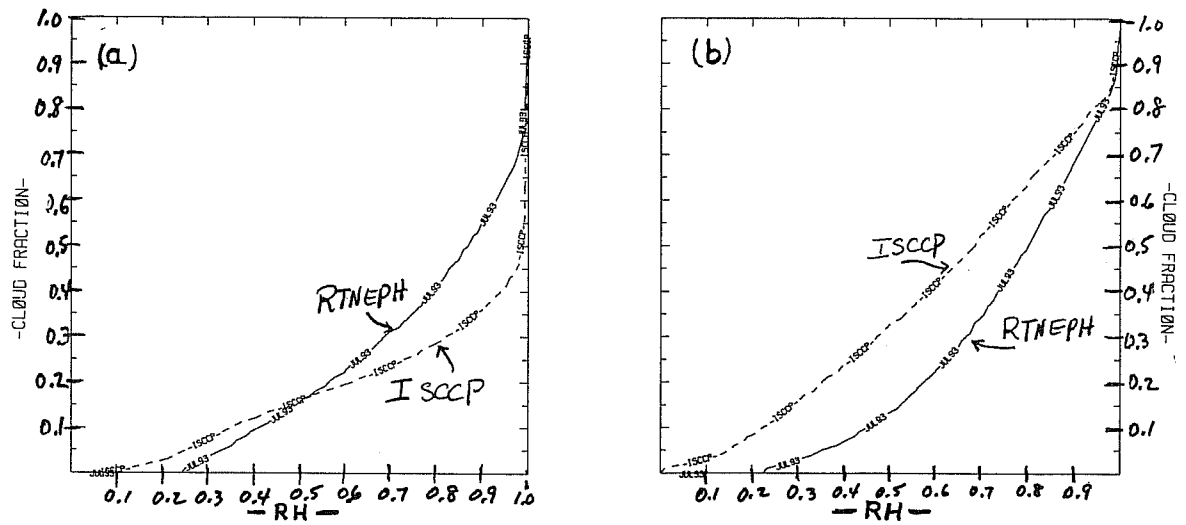

Fig. 11 Effect of cloud analysis – regional relationship between cloud fraction and model layer RH (abscissa) 'ISCCP (July 1985)/T62L18 model' (dashed) .vs. 'RTNEPH (July 1993)/T126L18 model' (solid) for low cloud, forecast day–1, Northern Hemisphere.
a) land b) ocean.

hemisphere for ISCCP (July 1985) and RTNEPH (July 1993). This is not surprising, since ISCCP has significantly more cloud, especially over ocean (Fig.1). Both are for an 18 layer vertical structure, but the ISCCP is for T62 and RTNEPH is for T126 resolution. Additional comparisons, not included in this paper, show that the relations derived from RTNEPH data do not change appreciably for MRF horizontal resolutions of T62 and T126, so Fig. 11 is an accurate portrayal of sensitivity to cloud analysis. Further examples of sensitivities, shown in Fig. 12, are due to surface type (Fig. 12a), to geographical region (Fig. 12b), and to vertical location (Fig. 12c–d). Seasonal effects may be large (Fig. 13), which appear to be reactions to realistic, physically plausible, changes in frequency distribution for both MRF layer–RH categories and RTNEPH cloud categories, *e.g.* the "wax and wane" of a convective signal. However, changing curves every month would result in a new initial data set for the MRF model. NMC has chosen a more conservative approach, merging the monthly data into a seasonal mean. To illustrate differences with the current operational cloud/RH relation, seasonal mean relationships for all geographical regions are merged into global curves in Figure 14. Here "critical" RH values for L, M, and H of 0.25, 0.4, and 0.5 over land and 0.15, 0.5, and 0.85 over ocean are significantly different than the 0.8 used everywhere in the current scheme. These seasonal curves are virtually identical to annual mean curves (not shown), so they provide a robust input to the MRF model. There is also a sensitivity to forecast day (Fig. 15), which in many regions is small (Fig. 15a), but in others can be larger (fig. 15b). The shift in the cloud curve in Fig. 15b is due to spinup in the MRF model RH.

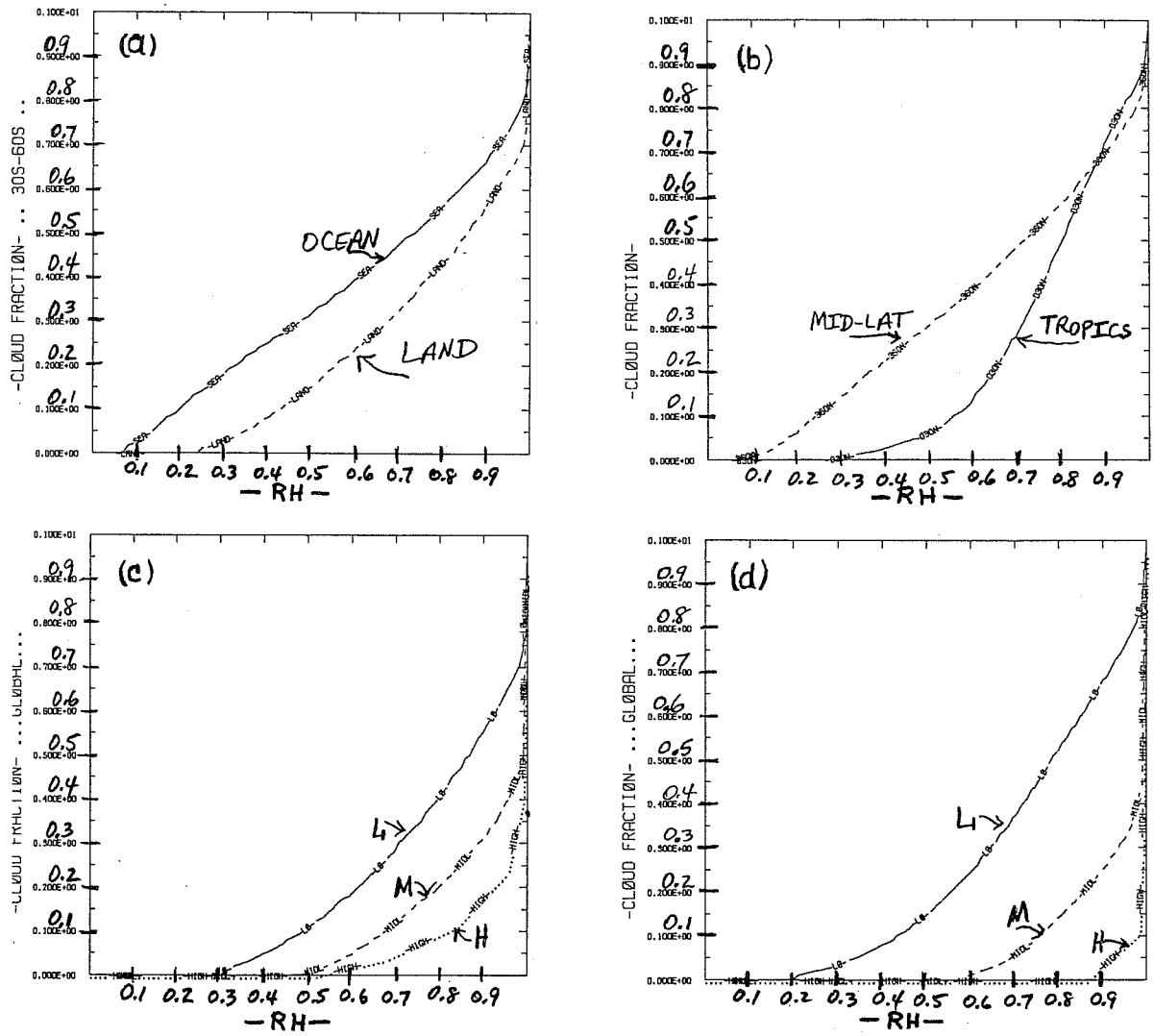

Fig. 12 Regional relationship between cloud fraction and model layer RH (abscissa) from RTNEPH and MRF T126L28 model for forecast day–5, October 1993.
a) ocean (solid) .vs. land (dashed), 30S–60S, low cloud, b) tropics (solid) .vs. mid–latitude (dashed), ocean, low cloud,
c) low (solid) domains, middle (dashed), high (dotted) global, land, d) same as c) for ocean.

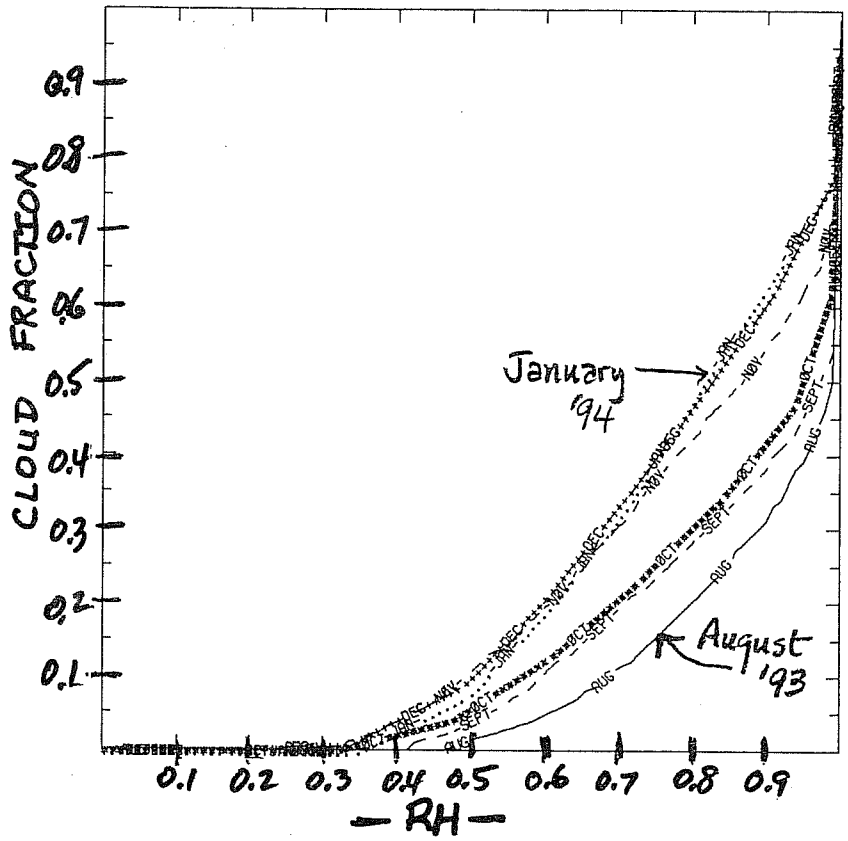

Fig. 13 Effect of seasonal change – regional relationship between cloud fraction and model layer RH (abscissa) from RTNEPH / T126L28 model for forecast day–1, middle cloud, Southern Hemisphere, land, for August 1993–January 1994 (6 curves).

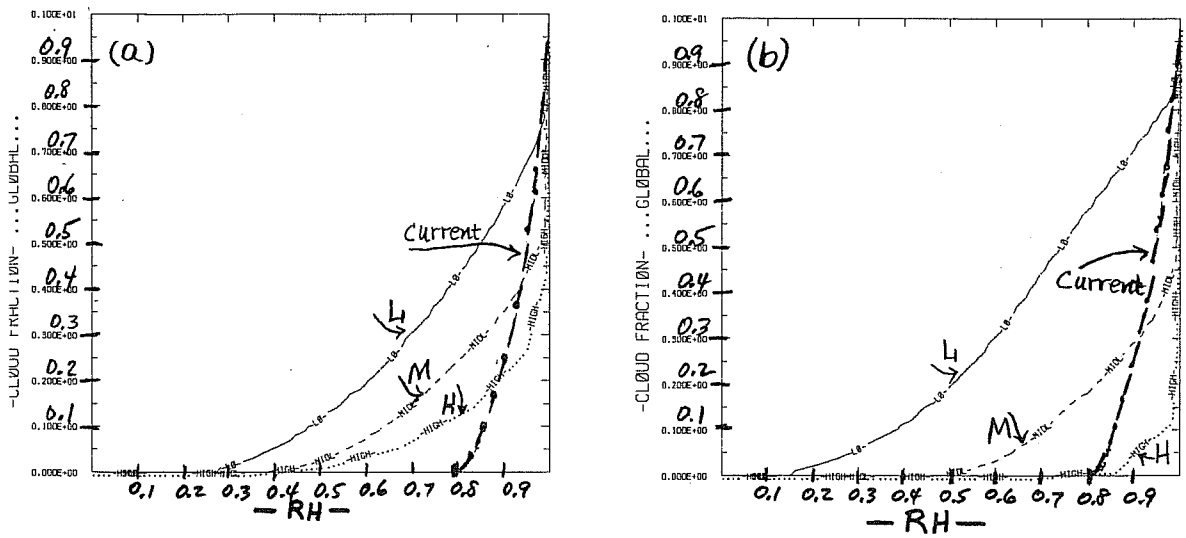

Fig. 14 Regional relationship between cloud fraction and model layer RH (abscissa) from RTNEPH/T126L28 model for forecast day–1, low (solid), middle (dashed), high (dotted) domains, global, seasonal mean of data from August 1993–February 1994. For reference, current quadratic curve is heavy dashed line emanating from RH = 0.8
a) land, b) ocean.

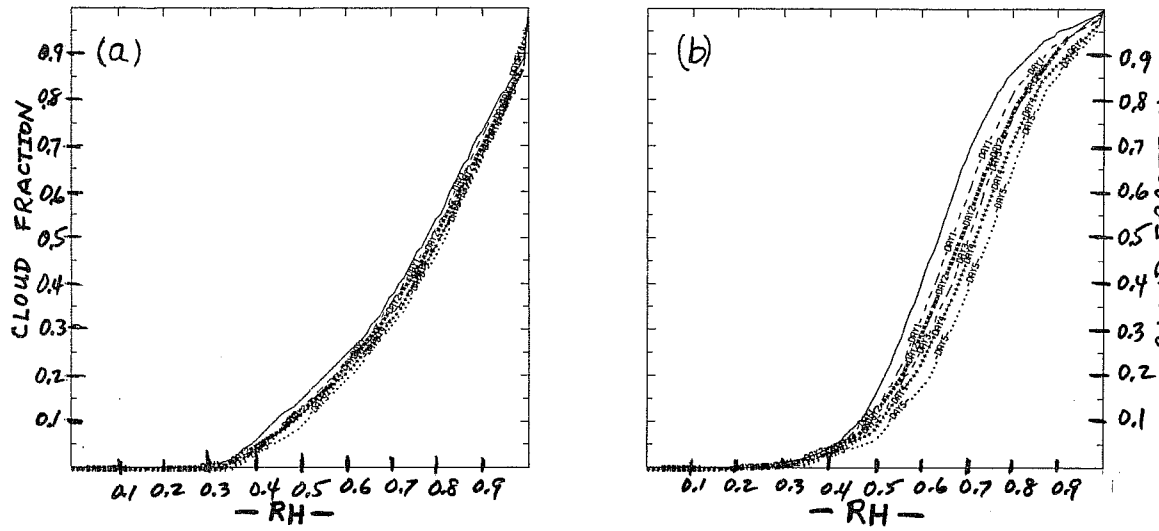

Fig. 15 Effect of forecast day – regional relationship between cloud fraction and model layer RH (abscissa) from RTNEPH / T126L28 model for 0–30N, low cloud, July 1994, forecast days 0–5 (6 curves). a) land, b) ocean.

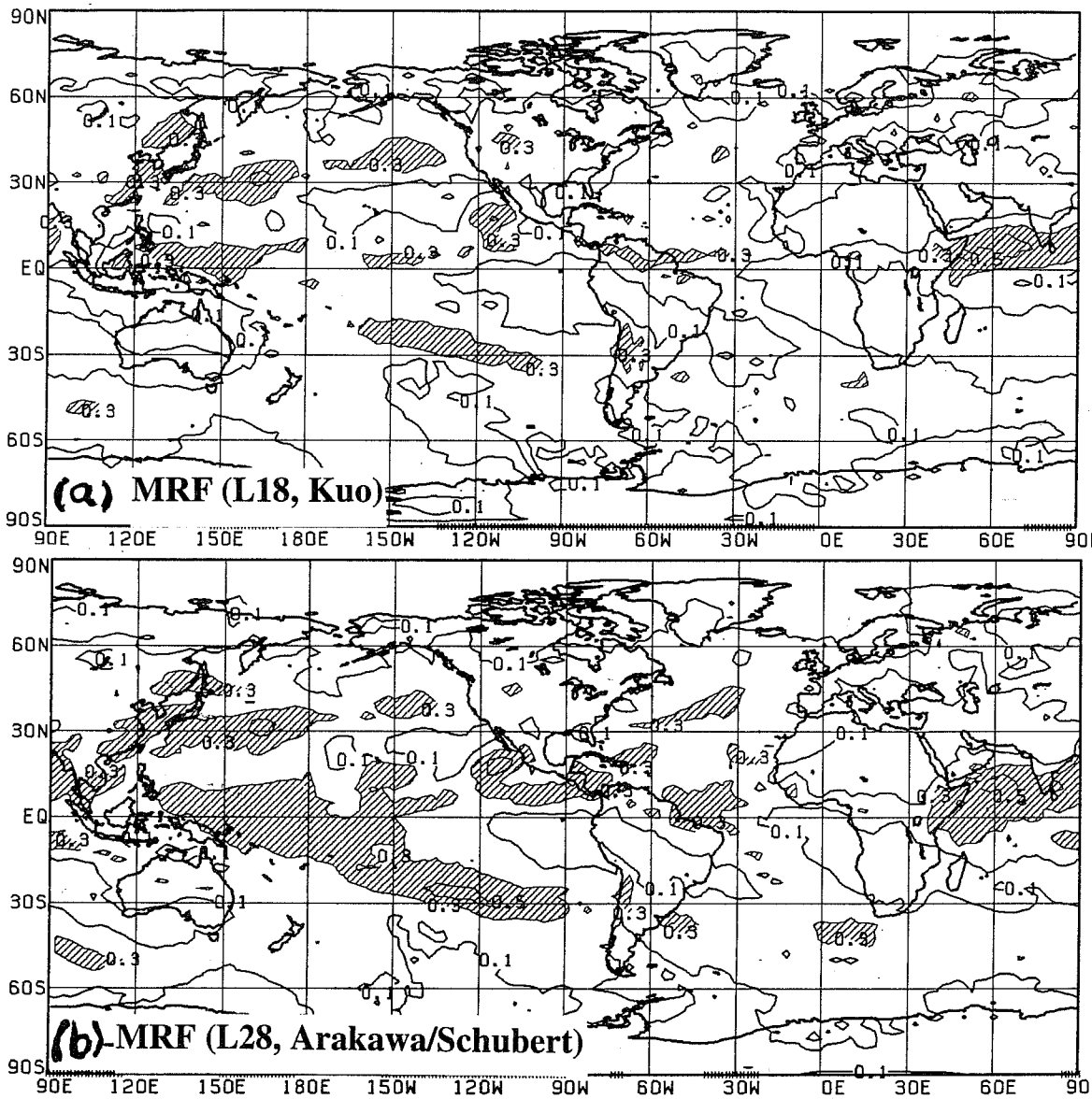

Fig. 16 Mean high cloud fraction for 1–16 June 1993 for T126 MRF model, forecast day–1, contour interval 0.2, shaded > 0.3
a) 18–layer model with Kuo parameterization,
b) 28–layer model with Arakawa/Schubert parameterization.

The tuning procedure will prove especially useful whenever changes are introduced into other components of the MRF which alter the moisture structure, and thus diagnosis of clouds. In the summer 1993, NMC changed the vertical structure of the model from 18 to 28 layers and changed its convective parameterization from Kuo to a modified Arakawa–Schubert scheme. Effects of the latter were seen in the RH structure of the model's upper tropical atmosphere, where values of RH increased by up to 25% in the zonal mean and showed commensurate increases in diagnosed H cloud (Fig 16). Cloud/RH curves developed from this new model, though not shown, changed for H cloud as they adjusted for a more moist upper atmosphere.

5. CHANGES TO THE CLOUD–RADIATION PARAMETERIZATION
(Y. Hou, K. Campana)

Here is a summary of changes (Campana et al., 1994b) which will be implemented in January 1995 into the diagnostic cloud parameterization of the operational T126 MRF model. Section 5.1, below, describes use of the material which was discussed in the preceding section, whereas sections 5.2–5.4 briefly describe additional changes not previously discussed. Together, these changes reduce deficiencies of the modeled clouds that were noted earlier. Parameterization adjustments are made to: a) the cloud/RH relationship, b) the vertical definition of clouds, c) the modeled convective cloud, and d) the cloud radiative properties. The low–level marine stratus component of the parameterization is not changed. Features of the new scheme are shown below:

5.1 **Cloud/RH Relationship:** The quadratic cloud/RH relation, with a fixed "critical" RH of 0.8, is replaced by a set of relationships accounting for several of the sensitivities noted in the previous section. Seasonal mean relations, developed from daily mean RTNEPH clouds, are for surface type (land, sea), for geographical region (tropics, mid–latitude) and for vertical domain. Though only the relationships for forecast day–1 are used, tests of the new clouds have shown that cloud spinup during the first 5 days is not as severe as in current model forecasts. Mid–latitude curves are used poleward of 60 degrees latitude, since polar region cloud analyses are very unreliable. There is ongoing investigation into possible use of continuously–tuned relationships, which would add an additional set of initial data for the model. In this case, sufficient data must be accumulated in order to produce stable cloud/RH relationships, either through use of large geographical regions or by accumulating the data for long–enough time periods (15 days appears to be sufficient). In most regions, the new relations significantly differ from the current quadratic relation (recall the illustrative global curves in Fig. 14).

5.2 **Vertical Structure (Fig. 17):** Cloud types are defined as groups of contiguous layers where cloud fraction is greater than zero. The current H, M, L cloud specification at the layer of maximum RH, with clouds thickened into adjacent cloudy layers, is no longer used. Thus, more than three "types" or groups of vertically–contiguous cloud may exist a point.

5.3 **Convective Cloud (Fig. 17):** Cloud fractions are obtained from a percentage of the Convective Coverage (CC), as calculated from the convective precipitation rate (Slingo, 1987); however, in the current scheme this produces very little middle atmosphere tropical cloud. The new scheme creates a columnar cloud from CC itself and permits existence of stratiform cloud in layers above and below the convection. If the convection is intense enough (rainfall rate) and deep enough, an anvil (Slingo, 1987) is placed in a single layer above the convection and is treated as a separate stratiform cloud.

5.4 **Radiative Properties:** Preset cloud radiative properties for each cloud type are replaced by those computed, for shortwave reflectance and transmittance and longwave emissivity, using parameterized optical depth of the cloud. The method, described by Harshvardhan et al. (1989), is based on theoretical and observational work. For cold (below freezing) supersaturation cloud, at least, there is a good relationship among cloud pressure thickness (Δp), SW optical depth, τ, and cloud temperature, T. The set of equations below are versions of Harshvardhan's, which have been altered in response to impacts on the thermal structure of the model atmosphere during preliminary, July–August 1985, tests of the NMC Reanalysis Project (Kistler, et al., 1994). Adjustments to the optical depth formulation evolved from collaborating with NMC's Development Division to alleviate too much lower atmospheric heating in summer high latitudes :

High and Convective cloud :

$$\text{For } T_i \leqq -10C \quad \tau_i = MAX\left(0.1 \times 10^{-3},\ 2 \times 10^{-6}\ (T_i + 82.5)^2\right) \Delta p_i$$

$$\text{For } T_i > -10C \quad \tau_i = MIN\left(0.08,\ 6.949 \times 10^{-3} T_i + 0.1\right) \Delta p_i \qquad (1)$$

Middle and Low cloud :

$$\text{For } T_i \leqq -20C \quad \tau_i = MAX\left(0.1 \times 10^{-3},\ 2.56 \times 10^{-5}(T_i + 82.5)^2\right) \Delta p_i$$

$$\text{For } T_i > -20C \quad \tau_i = 0.1\ \Delta p_i \qquad (2)$$

For clouds extending over more than 1 model layer, cloud optical depths are summed over *the 'i'* model layers. For SW reflection and transmission, the equations of Sagan and Pollack, 1967 are used (see equations 5.17, 5.18 in Paltridge and Platt, 1976). LW emittance is calculated as $1 - e^{-.75\tau}$.

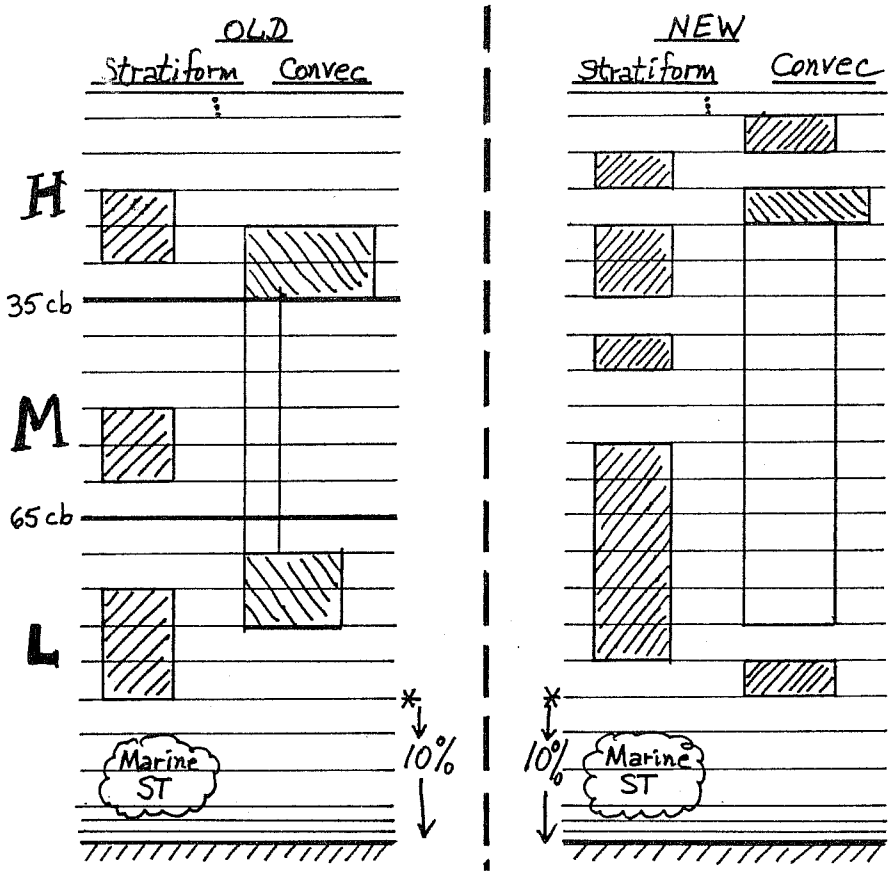

Fig. 17 Vertical schematic representation of MRF model diagnosed clouds – current operational, Autumn 1994 (left) .vs. new operational, January 1995 (right).

6. IMPACT OF CHANGES TO THE CLOUD–RADIATION PARAMETERIZATION

(K. Campana and R. Pinker, U of MD)

The new cloud scheme has been tested in a parallel–to–operations T126 mode. Impact of the new clouds is difficult to discern in the 2–dimensional pressure level data – *e.g.* anomaly correlations are quite similar. However, the impact is more obvious in the zonal mean model atmosphere, where temperature (and thus height) error is reduced. A warmer zonal model atmosphere is seen at forecast day–5, especially in the tropics (Fig. 18), which is responding to reduced LW cooling in the columnar convective cloud.

Comparison of physical cloud fields produced by the new cloud scheme, current cloud scheme (control), and RTNEPH for 15 days in May 1994, at forecast day–1, shows that the new clouds are significantly more accurate (Fig. 19), especially over land masses. Zonal mean comparison of model daily mean L, M cloud (Figs. 20–21) with the RTNEPH analysis shows improvement in M and L cloud in the tropics and generally in L at all latitudes (Fig. 20). Comparisons of H cloud, not included in this paper, show mixed results, which is partially due to inaccuracies in the computed RTNEPH–H cloud, itself. Forecast day–1 (as well as day–5) statistical comparisons show the improvement in low cloud 20/20 and correlation scores (Fig. 22a–b) and a significant reduction in the negative bias (Fig. 22c) in all regions. The sharp gradients between clear and overcast in the RTNEPH are not reproduced by the new scheme however, and contrast scores are lower than the control model in a number of regions (Fig. 22d). Developing tuned cloud/RH relationships from daily mean data may be a cause of the lower contrast scores. Tuning with individual synoptic data has produced a set of cloud curves (Fig. 23) which enhance these gradients and, at least for one case, show a slight increase in contrast score.

Comparison of radiative flux from the NMC T62 reanalysis (0Z, 6Z, 12Z, 18Z) of July 1985 also shows that the new cloud scheme is an improvement. Zonal monthly mean OLR for the new clouds is a better simulation, especially in the region of the ITCZ minimum, when compared with observed AVHRR OLR data (Fig. 24). Additional zonal mean comparisons of downward SW radiative flux at the earth's surface with Pinker and Laszlo's (1992) observational estimates also show general improvement for the new cloud test, especially in tropical and subtropical regions (Fig. 25). This is desirable for the NMC coupled Pacific Ocean model, where operational model overestimates of DSW, on the order of 50 W/m^2, has detrimental impact on predicted sea surface temperature. The overestimates of OLR near 30S and DSW in the 30–60N region are remaining problems which will be addressed in the future.

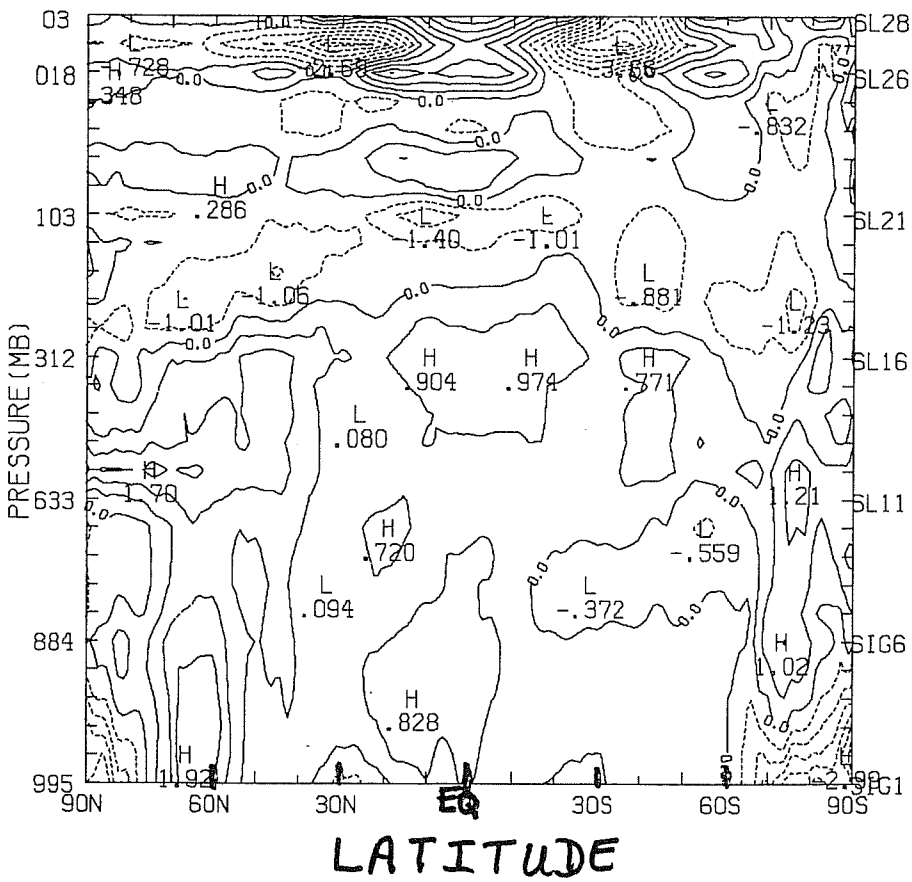

Fig. 18 Zonal mean temperature difference (deg K) for T126L28 MRF forecast day–5, (6–16) May 1994, (New–Current) cloud scheme. Contour interval=0.5K, negative values dashed, north pole at left.

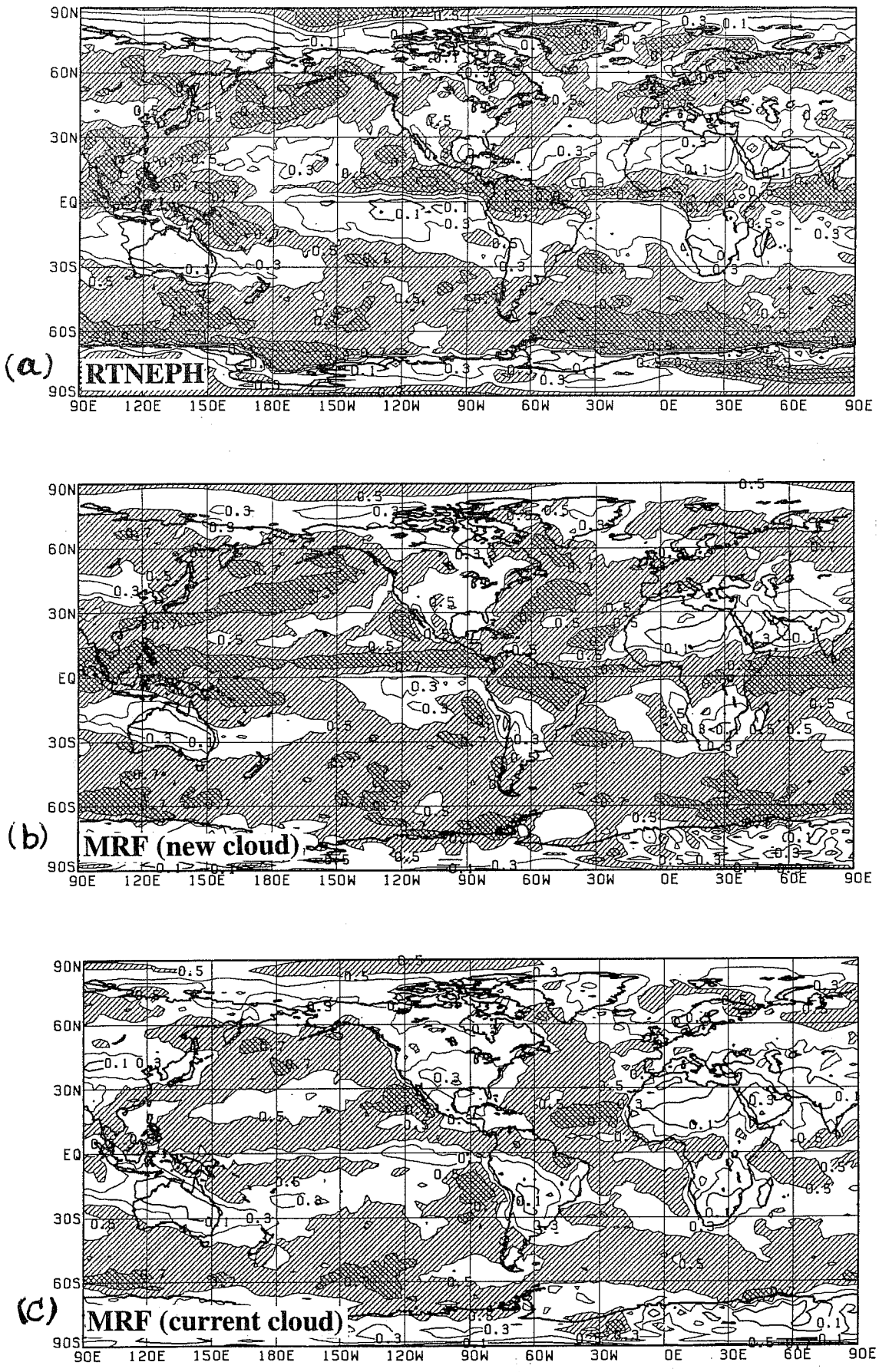

Fig. 19 Mean total cloud fraction for 12–27 May 1994 for T126L28 MRF model, forecast day–1, contour interval 0.2, shaded > 0.5, cross–hatched > 0.7
a) RTNEPH observed, b) MRF new cloud, c) MRF current cloud.

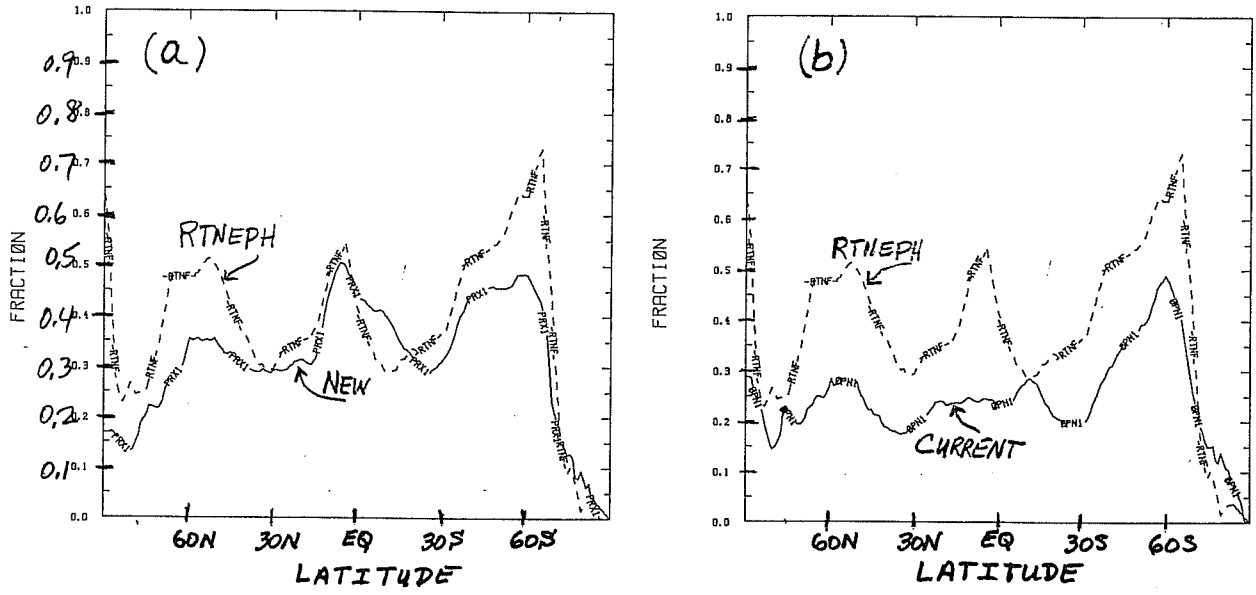

Fig. 20 Zonal mean low cloud fraction at forecast day–1, (12–27) May 1994, RTNEPH (dashed), MRF (solid).
a) new cloud, b) current cloud.

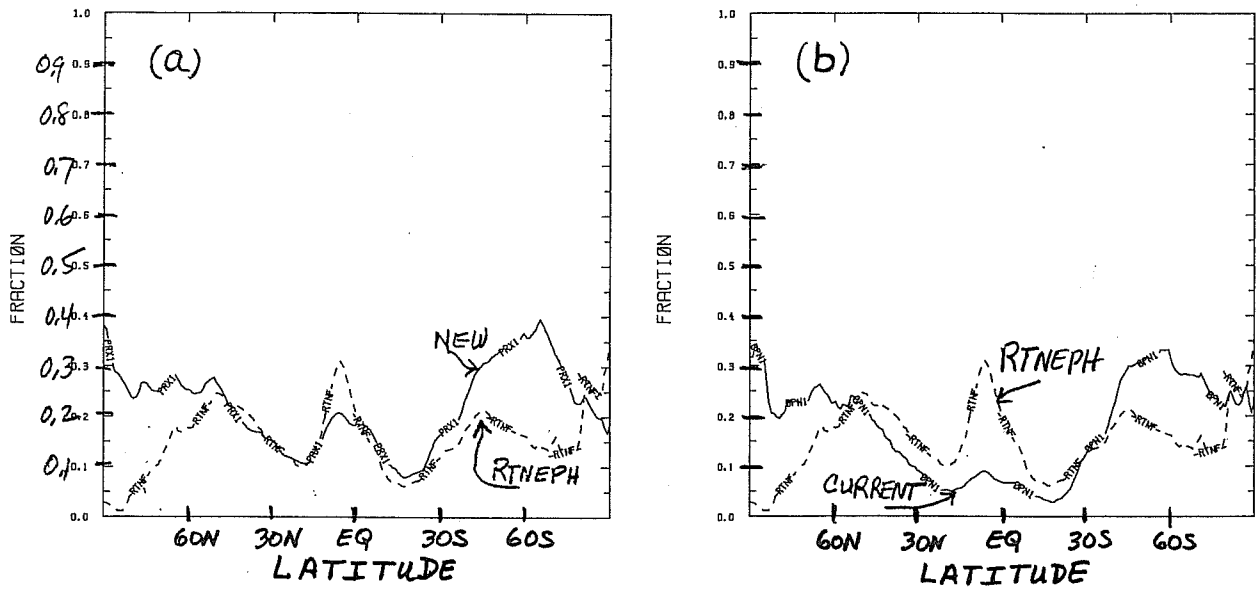

Fig. 21 Zonal mean middle cloud fraction at forecast day–1, (12–27) May 1994, RTNEPH (dashed), MRF (solid).
a) new cloud, b) current cloud.

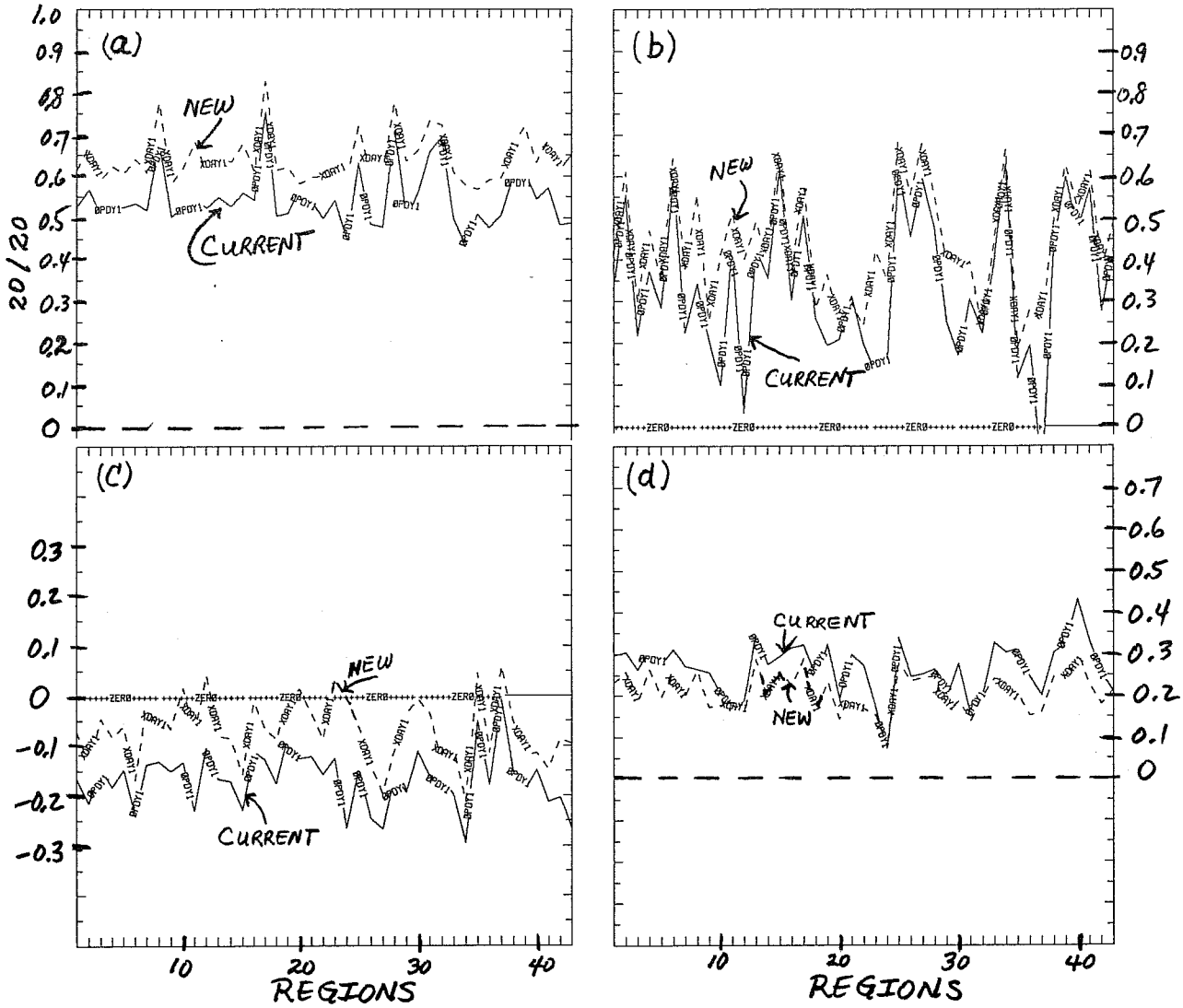

Fig. 22 Regional scores (43 regions) for MRF model (T126L28) .vs. RTNEPH daily mean low cloud for (12–27) May 1994, current cloud (solid), new cloud (dashed) – forecast day–1.
a) 20/20 Score, b) Correlation, c) Bias, d) Contrast.

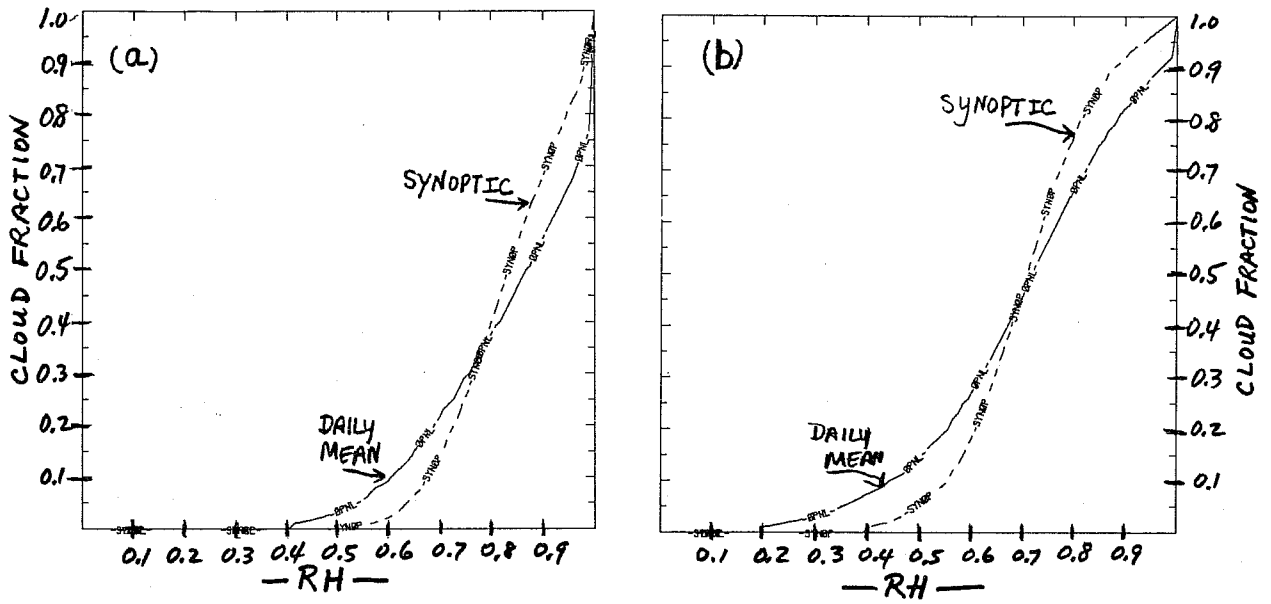

Fig. 23 Regional relationship between cloud fraction and model layer RH (abscissa) from RTNEPH/T126L28 model for forecast day–1, seasonal mean (January–August 1994), low cloud, 0–30S, RTNEPH daily mean (solid) .vs. RTNEPH 00Z synoptic (dashed).
a) land, b) ocean.

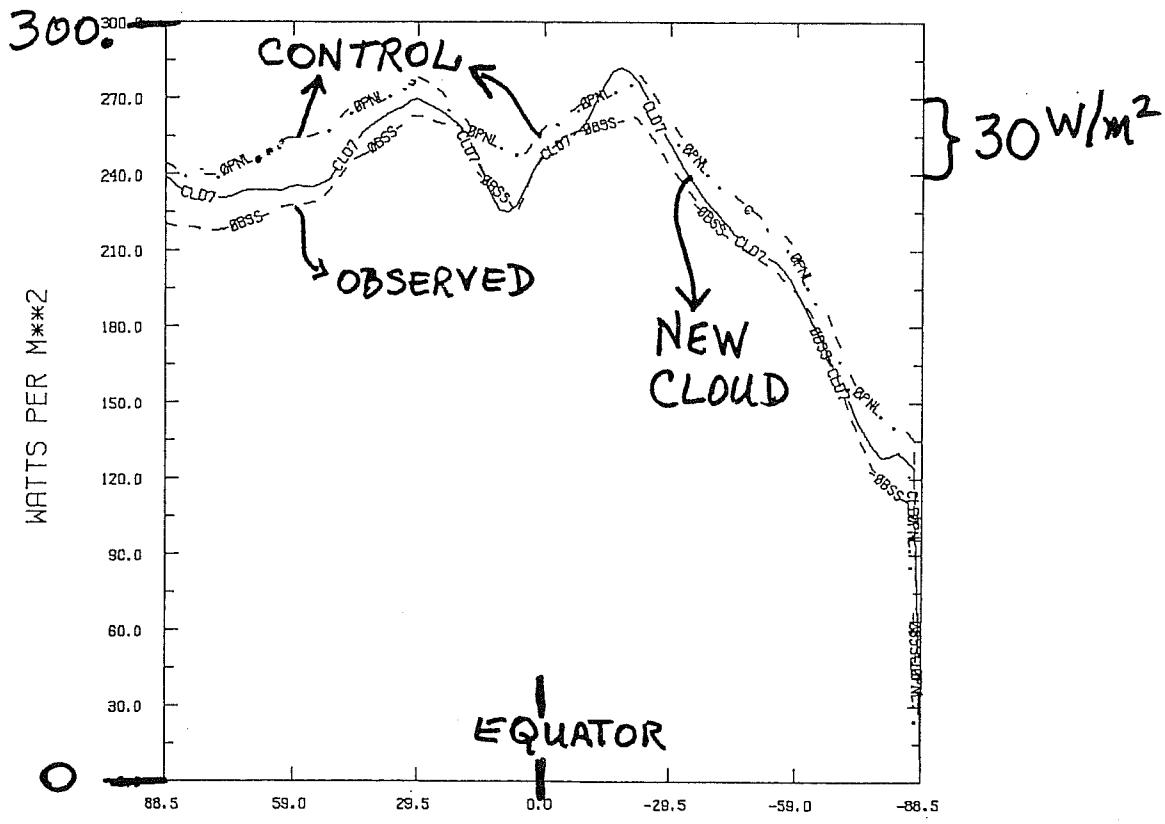

Fig. 24 Zonal mean OLR (0.–300. W/m^2), north pole at left, observed (AVHRR) .vs. current (labeled "control") .vs. new cloud (solid line), July 1985, T62L28 reanalysis mean of data at 0Z, 6Z, 12Z, 18Z.

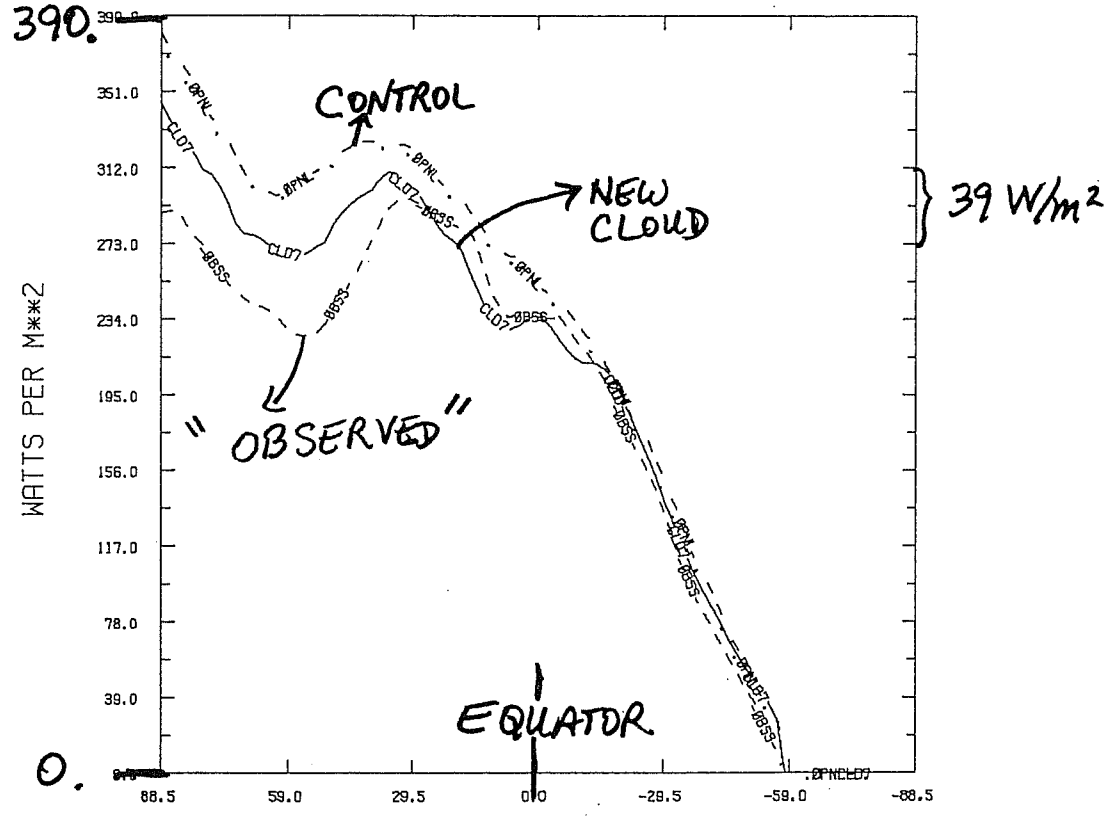

Fig. 25 Zonal mean DSW (0.–390. W/m^2), north pole at left, observed (Pinker–Laszlo,1992) .vs. current (labeled "control") .vs. new cloud (solid line), July 1985, T62L28 reanalysis mean of data at 0Z, 6Z, 12Z, 18Z.

7. ACKNOWLEDGEMENTS

This work would not have been possible without the combined efforts of the people acknowledged at the beginning of each section. Special thanks to Yu–Tai Hou who was invaluable in just about every facet of this work – *e.g.* the CLAVR data, the code used to calculate the variety of cloud scores, and many of the changes to the cloud parameterization. In addition, the author wishes to thank S. Fels and D, Schwarzkopf, GFDL, who, over the last 10 years have graciously provided NMC with the latest versions of GFDL's LW and SW radiation parameterizations, R. Pinker, U. of Maryland, who produced satellite estimates of downward SW fluxes, M. Ji, NMC, who developed the compressed RTNEPH archive, making the validation and tuning work feasible, R. Kistler S. Saha, and M. Kanamitsu, NMC, who tested the new clouds in the NMC Reanalysis Project, and K. Mitchell, who provided a very valuable, thorough review of this report.

8. REFERENCES

Black, T. L., 1994: The new NMC mesoscale Eta model: description and forecast examples, *Weather and Forecasting*, **9**, 265–278.

Campana K. A., 1990: Radiation and cloud parameterization at the National Meteorological Center, ECMWF/WCRP Workshop on Clouds, Radiation, and the Hydrological Cycle, Reading U. K., 313–340.

Campana, K. A., P. M. Caplan, G. H White, S–K Yang, and H–M Juang, 1990: Impact of changes to cloud parameterization on the forecast error of NMC's global model, *7th AMS Conference on Atmospheric Radiation*, San Francisco CA, J152–J158..

Campana, K. A., Y. Hou, B. Balasubramaniyan, R. T. Pinker, and I. Laszlo, 1994a: Evaluation of NWP–computed SW radiative fluxes against satellite retrievals, *8th AMS Conference on Atmospheric Radiation,* Nashville TN.

Campana K. A., Y–T Hou, K. E. Mitchell, S–K Yang, and R. Cullather, 1994b: Improved diagnostic cloud parameterization in NMC's global model, *10th AMS Conference on Numerical Weather Prediction*, Portland OR, 324–325.

Cullather, R. I., 1993: An analysis of the cloud and radiation fields in the NMC medium–range forecast model, Master's Thesis, Purdue University, West Layfayette, IN.

DiMego, G. J., K. E. Mitchell, R. A. Peterson, J. E. Hoke, J. P. Gerrity, J. J. Tuccillo, R. L. Wobus, and H–M Juang, 1992: Changes to NMC's regional analysis and forecast system, *Weather and Forecasting*, **7**, 185–198.

Dorman, J. L. and P. J. Sellers, 1989 : A global climatology of albedo, roughness length and stomatal resistance for atmospheric general circulation models as represented by the simple biosphere model (SiB), *J. of Appl. Meteor.*, **28**, 833–855.

Hamill, T. M., R. P. d'Entremont, and J. T. Bunting, 1992: A description of the Air Force real–time nephanalysis model, *Weather and Forecasting*, **7**, 288–306.

Harshvardhan, D. A. Randall, T. G. Corsetti, and D. A. Dazlich, 1989: Earth radiation budget and cloudiness simulations with a general circulation model, *J. Atmos. Sci.*, **46**, 1922–1942.

Heck P. W. and B. J. Byars, D. F. Young, P Minnis, and E. F. Harrison, 1990: A climatology of satellite–derived cloud properties over marine stratocumulus regions, *7th AMS Conference on Atmospheric Radiation*, San Francisco CA, J1–J7..

Hou, Y–T., K. A. Campana, K. E. Mitchell, S–K. Yang, and L. L. Stowe, 1993: Comparison of an experimental NOAA AVHRR cloud dataset with other observed and forecast cloud datasets, *J. Atmos. and Oceanic Tech.*, **10**, 833–849.

Kalnay, E., M. Kanamitsu, and W. E. Baker, 1990: Global Numerical Weather Prediction at the National Meteorological Center. *Bull. Amer. Meteor. Soc.*, **71**, 1410–1428.

Kanamitsu, M., J. C. Alpert, K. A. Campana, P. M. Caplan, D. G. Deavan, M. Iredell, B. Katz, H–L Pan, J. Sela, and G. W. White, 1991: Recent changes implemented into the global forecast system at NMC, *Weather and Forecasting*, **6**, 425–435.

Kistler, R., M. Kanamitsu, and E. Kalnay, 1994: Overview of the NMC/NCAR reanalysis system, *10th AMS Conference on Numerical Weather Prediction*, Portland OR, 279–280.

Lacis, A. A. and J. E. Hansen, 1974: A parameterization for the absorption of solar radiation in the earth's atmosphere, *J. of Atmos. Sci.*, 118–133.

Manabe, S. and R. F. Strickler, 1964: Thermal equilibium of the atmosphere with a convective adjustment, *J. of Atmos. Sci.* **21**, 361–385.

McMillin, L. M., S–S Zhou, and S–K Yang, 1994: An improved cloud retrieval algorithm using HIRS2–MSU radiance measurements, *J. Appl. Meteor.*, **33**, 195–211.

McPherson, R. D., 1994: The national centers for environmental prediction: operational climate, ocean, and weather prediction for the 21st century, *Bull. Amer. Meteor. Soc.*, **75**, 363–373.

Mitchell, K. E. and D. C. Hahn, 1989: Development of a cloud forecast scheme for the GL baseline global spectral model, GL–TR–89–0343, Geophysics Laboratory, Hanscom AFB, MA.

Mitchell, K. E. and D. C. Hahn, 1990: Objective development of diagnostic cloud forecast schemes in global and regional models, *7th AMS Conference on Atmospheric Radiation*, San Francisco CA, J138–J145..

Mokhov, I. I. and M. E. Schlesinger, 1994: Analysis of global cloudiness, 2, comparison of ground–based and satellite–based cloud climatologies, *J. of Geophys. Res.*, **99**, **D8**, 17045–17065.

Nehrkorn, T. and M. Zivkovic, 1994: Development and testing of a cloud forecast scheme, *10th AMS Conference on Numerical Weather Prediction*, Portland OR, 133–134.

Paltridge, G. W. and C. M. R. Platt, 1976: *Radiative Processes in Meteorology and Climatology*, Developments in Atmospheric Science 5, Elsevier Scientific Publishing Company, 318 p.

Payne, R. E., 1972: Albedo of the sea surface, *J. of Atmos. Sci.*, 959–970.

Pinker, R. T. and I. Laszlo, 1992: Modeling surface solar irradiance for satellite applications on a global scale. *J. Appl. Meteor.*, **31**, 194–211.

Rikus, L. and T. Hart, 1988: The development and refinement of a diagnostic cloud parameterization scheme for the BMRC global model, *Proceedings of the International Radiation Symposium*, Lille, France.

Roberts, R., J. Selby, and L. Biberman, 1976: Infrared continuum absorption by atmospheric water vapor in the 8–12 μ window, *Applied Optics*, 2085–2090.

Rodgers, C. D., 1968: Some extensions and applications of the new random model for molecular band transmission, *Quart. J. of Roy. Meteor. Soc.*, 99–102.

Sagan, C. and J. B. Polack, 1967: Anisotropic nonconservative scattering and the clouds of Venus, *J. of Geophys. Res.*, **72**, 469–477.

Sasamori, T., J. London, and D. Hoyt, 1972: *Radiation budget of the southern hemisphere, Meteorological Monographs*, **13**, number **35**, 9–23.

Schiffer, R. A. and W. B. Rossow, 1985: ISCCP global radiance data set: A new resource for climate research. *Bull. Amer. Meteor. Soc.*, **66**, 1498–1505.

Schwarzkopf, M. D., and S. B. Fels, 1985: Improvements to the algorithm for computing CO_2 transmissivities and cooling rates, *J. of Geophys. Res.*, 10541–10550.

Schwarzkopf, M. D., and S. B. Fels, 1991 : The simplified exchange method revisited: An accurate, rapid method for computation of infrared cooling rates and fluxes, *J. of Geophys. Res.*, **96**, **D5**, 9075–9096.

Slingo, J. M., 1987: The development and verification of a cloud prediction scheme for the ECMWF model. *Quart. J. Roy. Meteor. Soc.*, **113**, 899–927.

Stowe, L. L., 1991: Cloud and aerosol products at NOAA/NESDIS, *Global and Planetary Change*, **4**, No. 1–3, 25–32.

Trapnell, R. N., 1992: Cloud curve algorithm test program, *Report PL–TR–92–2052*, Phillips Laboratory, Hanscom AFB, MA, 170 pp.

Zhao, Q., 1994: Prognostic cloud modeling at NMC, ECMWF/GEWEX Workshop on Modelling, Validation and Assimilation of Clouds, Reading U. K., paper found elsewhere in these Proceedings.